JGR Biogeosciences

RESEARCH ARTICLE
10.1029/2024JG008508

Increased Ecosystem Productivity Boosts Methane Production in Arctic Lake Sediments

Marie Bulínová[1], Anders Schomacker[1], Sofia E. Kjellman[1], Cristian Gudasz[2], Carolina Olid[3], Johan Rydberg[2], Giuliana Panieri[1], Andrew Hodson[4,5], Willem G. M. van der Bilt[6], Torgeir Opeland Røthe[5], Richard Bindler[2], and Alexandra Rouillard[1,2,7]

[1]Department of Geosciences, UiT The Arctic University of Norway, Tromsø, Norway, [2]Department of Ecology, Environment and Geoscience, Umeå University, Umeå, Sweden, [3]Department of Earth and Ocean Dynamics, UB-Geomodels Research Institute, University of Barcelona, Barcelona, Spain, [4]Department of Arctic Geology, The University Centre in Svalbard (UNIS), Longyearbyen, Norway, [5]Department of Civil Engineering and Environmental Sciences, Western Norway University of Applied Sciences, Sogndal, Norway, [6]Department of Earth Science and the Bjerknes Centre for Climate Research, University of Bergen, Bergen, Norway, [7]Umeå Marine Sciences Centre, Umeå University, Norrbyn, Sweden

Abstract Global estimates of methane (CH_4) emissions from lakes to the atmosphere rely on understanding CH_4 processes at the sediment-water interface (SWI). However, in the Arctic, the variability, magnitude, and environmental drivers of CH_4 production and flux across the SWI are poorly understood. Here, we estimate CH_4 diffusive fluxes from the sediment into the water column in 10 lakes in Arctic Scandinavia and Svalbard using porewater modeling and mass transfer estimates, which we then compare with 60 published estimates from the Arctic to the tropics. Diffusion of CH_4 in the sampled lake sediments ranged from −0.46 to 3.1 mmol m^{-2} day^{-1}, which is consistent with previous reports for Arctic and boreal lakes, and lower than for temperate and tropical biomes. Methane production occurs primarily within the top ∼10 cm of sediment, indicating a biogenic origin. Random forest predictive modeling of the sampled lakes revealed that conditions promoting production and deposition of autochthonous organic carbon in Arctic lakes drive CH_4 diffusion into the water column by fueling sediment CH_4 production. For small lakes across biomes, determinants of the estimated CH_4 flux were also best captured by climate predictors, with warmer and wetter conditions favoring ecosystem productivity and enhancing flux but also lake morphometry resulting in important regional variability in estimates. Our study emphasizes the importance of quantifying diffusive CH_4 fluxes from sediments in diverse lake types to account for differences in the controls on primary production and the preservation of organic carbon across and within different biomes, to refine CH_4 emission estimates in a warming climate.

Plain Language Summary Methane is a powerful greenhouse gas. Lakes in the Arctic release large amounts of methane to the atmosphere, which increases global warming. This study explores how methane moves from the sediments (accumulated layers of mud and organic matter) of Arctic lakes, where it is produced, into the overlying water. We find that most lakes release methane from their sediments, with some lakes having higher-than-expected methane levels, especially further north. The results from our advanced data analysis techniques suggest that carbon content in the water and sediment, lake depth and size, and latitude and elevation all influence methane production and release. Overall, we highlight the need to study methane dynamics from a wider variety of lakes to better understand and predict how methane is produced and released in different environments.

Key Points:

- We quantified the diffusive methane flux and determined the depth of biogenic methane production in the sediments of 10 Arctic lakes
- Regional methane flux variability in Arctic lakes relates to production and preservation of autochthonous organic matter
- Lake morphometry and climate are important predictors of methane diffusive flux from the sediment for small lakes across biomes

Supporting Information:

Supporting Information may be found in the online version of this article.

Correspondence to:

M. Bulínová,
marie.bulinova@uit.no

Citation:

Bulínová, M., Schomacker, A., Kjellman, S. E., Gudasz, C., Olid, C., Rydberg, J., et al. (2025). Increased ecosystem productivity boosts methane production in Arctic lake sediments. *Journal of Geophysical Research: Biogeosciences*, *130*, e2024JG008508. https://doi.org/10.1029/2024JG008508

Received 28 SEP 2024
Accepted 1 JUL 2025

Author Contributions:

Conceptualization: Marie Bulínová, Anders Schomacker, Giuliana Panieri, Alexandra Rouillard
Funding acquisition: Marie Bulínová, Anders Schomacker, Andrew Hodson, Willem G. M. van der Bilt, Alexandra Rouillard
Investigation: Marie Bulínová, Anders Schomacker, Sofia E. Kjellman, Carolina Olid, Andrew Hodson, Willem G. M. van der Bilt, Torgeir Opeland Røthe, Alexandra Rouillard
Methodology: Marie Bulínová, Cristian Gudasz, Carolina Olid, Johan Rydberg, Giuliana Panieri, Alexandra Rouillard
Resources: Anders Schomacker, Johan Rydberg, Giuliana Panieri, Richard Bindler
Software: Marie Bulínová, Alexandra Rouillard

1. Introduction

With their large coverage of the regional land surface (Downing et al., 2006), Arctic lakes represent a major natural source of atmospheric greenhouse gases (Lauerwald et al., 2023). Among these, methane (CH_4) is particularly potent, with a warming potential approximately 27 times than that of carbon dioxide (CO_2) over a centennial timescale (Forster et al., 2021). Because Arctic lakes are located in one of the most rapidly warming regions on Earth (Rantanen et al., 2022), they are expected to experience shifts in ecosystem functioning—changes that are already being observed (IPCC, 2021; Wik et al., 2016). These changes could enhance carbon processing and CH_4 emissions (Fowler et al., 2020; Kuhn et al., 2021; McGowan et al., 2016), contributing to

Supervision: Anders Schomacker, Giuliana Panieri, Alexandra Rouillard
Visualization: Marie Bulínová, Anders Schomacker, Sofia E. Kjellman, Alexandra Rouillard
Writing – original draft: Marie Bulínová, Anders Schomacker, Alexandra Rouillard
Writing – review & editing: Marie Bulínová, Anders Schomacker, Sofia E. Kjellman, Cristian Gudasz, Carolina Olid, Johan Rydberg, Giuliana Panieri, Andrew Hodson, Willem G. M. van der Bilt, Torgeir Opeland Røthe, Richard Bindler, Alexandra Rouillard

strong positive climate feedbacks (Schuur et al., 2015). Yet, the sensitivity of CH_4 emissions from Arctic lakes to climate change is still uncertain due to a poor understanding of the underlying controlling processes of such emissions (Aben et al., 2017; Hastie et al., 2018). A key step toward resolving this uncertainty is a deeper investigation into CH_4 production in sediments, as it is a primary driver of emissions (Jansen et al., 2020). Even though CH_4 oxidation and other removal pathways play an important role for the net emissions (Bastviken et al., 2003), it is the rate and magnitude of CH_4 production that ultimately set the upper limit for emissions. Therefore, understanding the environmental and biogeochemical factors that control CH_4 production in lake sediments is crucial for predicting future CH_4 fluxes and their role in future climate feedback.

Production of CH_4 in lakes primarily occurs in the sediments, where organic matter (OM) accumulates and undergoes microbial degradation (Gudasz et al., 2010; Peeters et al., 2019). Although whole-lake CH_4 emissions have been widely studied, the specific environmental drivers regulating CH_4 production in lake sediments are not well constrained. Incubation studies have provided valuable insights into the key drivers of methanogenesis and methane consumption in northern lake sediments (e.g., Bretz & Whalen, 2014; Carnevali et al., 2015; de Jong et al., 2018; Duc et al., 2010; Gentzel et al., 2012; Heslop et al., 2019; Lofton et al., 2014; Pellerin et al., 2022). However, the variability in environmental drivers under natural conditions remains poorly understood (Cunada et al., 2018).

Temperature is a well-established driver of CH_4 production in freshwater sediments, with studies demonstrating a positive exponential correlation between CH_4 production and temperature (Duc et al., 2010; Yvon-Durocher et al., 2014). Additionally, in-lake OM production and its subsequent delivery to the sediments have been closely connected with sediment CH_4 production (Isidorova et al., 2019; Moras et al., 2024). However, sediment CH_4 production and its associated production pathways (e.g., acetoclastic and hydrogenotrophic methanogenesis) depend not only on OM supply but also on its degradability (Grasset et al., 2018, 2021; Schwarz et al., 2008; West et al., 2012, 2015), redox conditions (Van Grinsven et al., 2022), deposition of fine-grained material (Bodmer et al., 2020), and sediment depth (Wilkinson et al., 2015). A meta-analysis of over 60 lakes and reservoirs suggested that sediment CH_4 production rates could be linked to trophic status (D'Ambrosio & Harrison, 2021; DelSontro et al., 2018). Lake trophic status may be disconnected from the fraction of OM available in sediments for fueling CH_4 production. This fraction is influenced not only by processes controlling primary production (PP) but also by those governing OM transport and degradation, such as thermal stratification regimes, convective mixing, and biological uptake. Furthermore, it remains unclear whether trophic status would have the same impact in clear and shallow high-latitude lakes, where productivity is low, and ice cover persists for extended periods. In these systems, gross PP predominantly occurs near the lake bottom, particularly in soft sediments, which are also the primary sites of CH_4 production.

Understanding whether the same drivers of CH_4 production observed in lower-latitude lakes apply to high-latitude systems is essential for improving predictions of CH_4 emissions in a warming Arctic. One approach to do this is modeling of chemical processes in the sediments. This can reveal down-profile variability in various processes related to CH_4 production, degradation and diffusion, and thus contribute to a more mechanistic understanding of the drivers for CH_4 fluxes in sediments. In this study, we aim to determine environmental drivers and variability of CH_4 production in high-latitude lakes. With this objective, we measured CH_4 concentration and indicators of ecosystem productivity in sediments (i.e., autochthonous and terrestrial OM inputs), as well as morphometric and landscape properties from 10 Arctic lakes. We then applied porewater diffusion modeling, mass transfer estimates, and random forest (RF) predictive modeling on the sampled lakes to (a) establish a baseline of CH_4 diffusive fluxes across the sediment-water interface (SWI) from Arctic lakes; (b) determine the depth of CH_4 production; (c) identify predictive variables of the diffusive CH_4 flux across the SWI from the sedimentological, morphometric, hydrological, and catchment measurements; then (d) develop a predictive model of diffusive CH_4 fluxes across the SWI including published data from an additional 60 lakes.

2. Materials and Methods

2.1. Regional Setting and Study Sites

The 10 lakes sampled in this study included three lakes from High Arctic Svalbard and seven from Subarctic Scandinavia (Figure 1; Figure 2; Table 1). The area of the lakes ranges from 0.015 to 0.11 km^2 and the lakes are generally shallow (maximum depth between 4.1 and 8.6 m) except for Stuptjørna in Svalbard (maximum depth

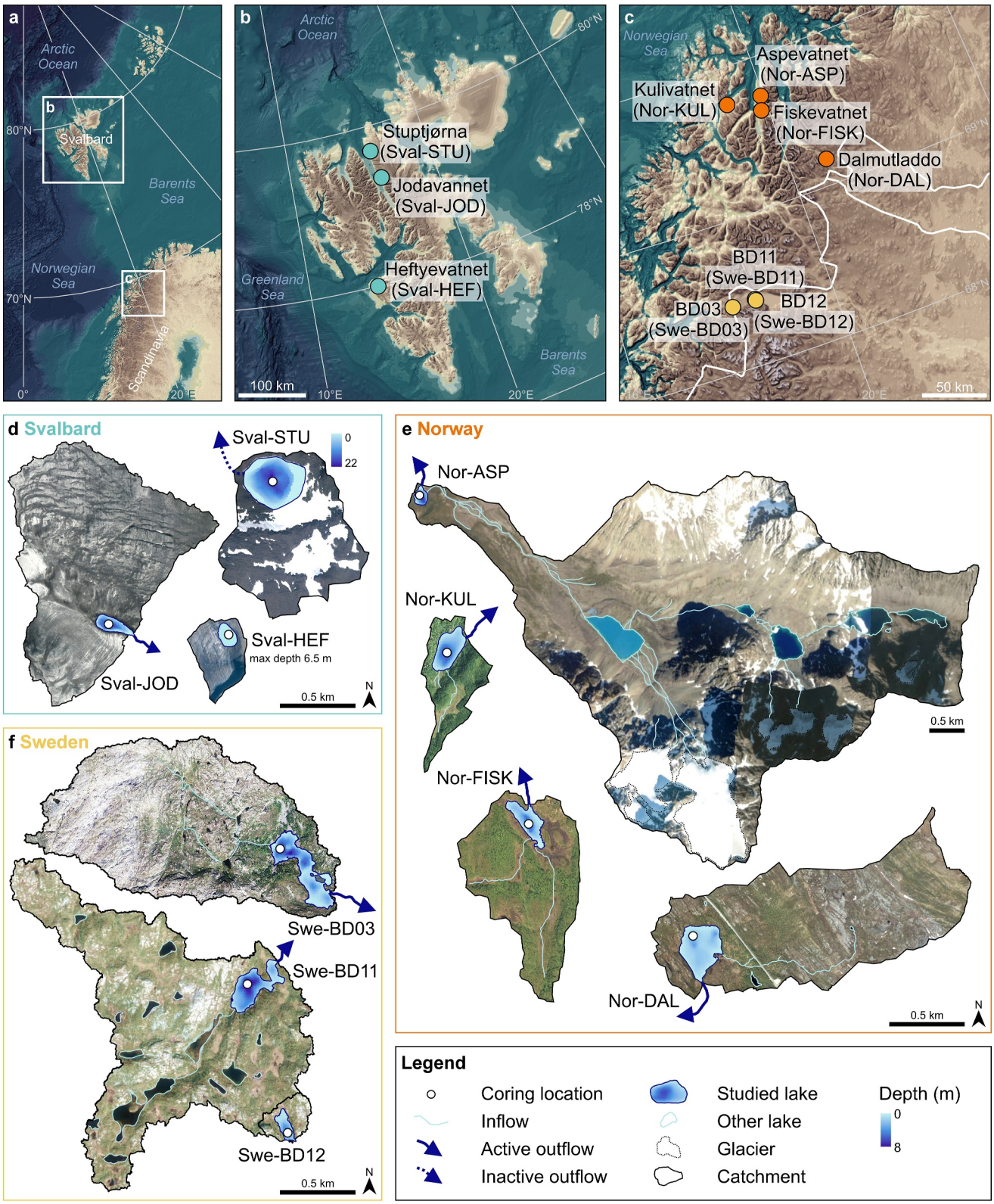
a
Arctic Ocean
b
Svalbard
80°N
Barents Sea
Norwegian Sea
c
70°N
Scandinavia
0°
20°E
b
Arctic Ocean
80°N
Stuptjørna (Sval-STU)
Jodavannet (Sval-JOD)
78°N
Heftyevatnet (Sval-HEF)
Greenland Sea
Barents Sea
100 km
10°E
20°E
c
Norwegian Sea
Aspevatnet (Nor-ASP)
Kulivatnet (Nor-KUL)
Fiskevatnet (Nor-FISK)
69°N
Dalmutladdo (Nor-DAL)
BD11 (Swe-BD11)
BD03 (Swe-BD03)
BD12 (Swe-BD12)
68°N
16°E
20°E
50 km
d Svalbard
Sval-STU
0
22
Sval-HEF
max depth 6.5 m
Sval-JOD
0.5 km
N
e Norway
Nor-ASP
Nor-KUL
Nor-FISK
Nor-DAL
0.5 km
N
f Sweden
Swe-BD03
Swe-BD11
Swe-BD12
0.5 km
N
Legend
Coring location
Inflow
Active outflow
Inactive outflow
Studied lake
Other lake
Glacier
Catchment
Depth (m)
0
8

Figure 1.

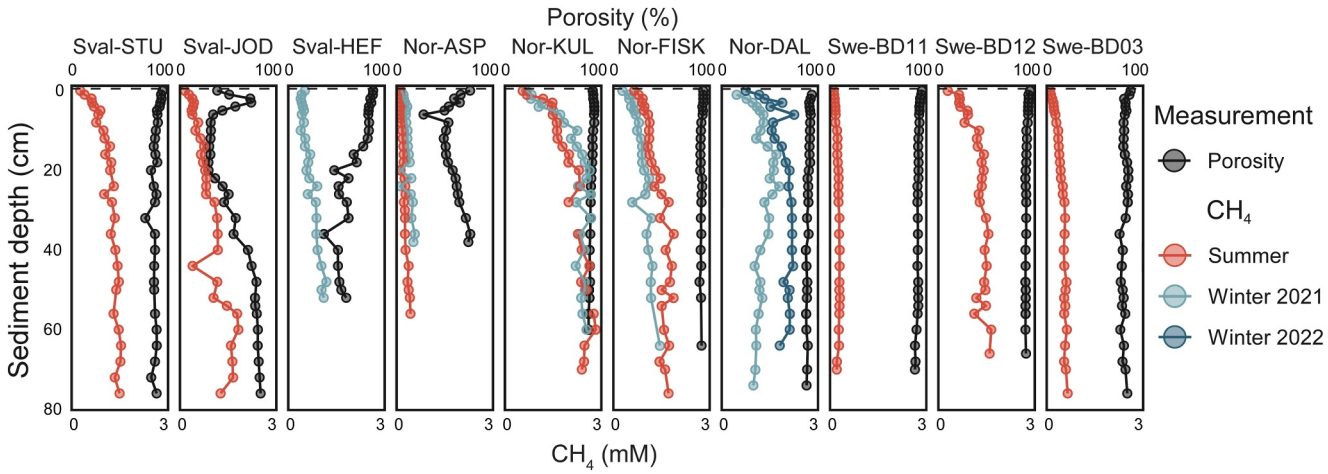

Figure 2. Downcore profiles of [CH_4] and porosity measurements at the 10 Arctic lakes sampled. The sediment-water interface is at 0 cm (gray dashed line). Summer sampling is represented with orange symbols, winter sampling with blue symbols. Two shades of blue were introduced to differentiate between 2 years of winter sampling. Porosity is represented with black symbols.

22.6 m). The lakes are oligotrophic with clear to slightly colored water (indicating higher dissolved organic carbon; DOC). All lakes are seasonally ice covered. Thermal regimes and oxygen cycles in the lakes are not well defined; however, oxygen depletion in the bottom water is expected to occur when the lakes are ice covered (Leppi et al., 2016), whereas well-mixed oxygenated water columns exist during the brief ice-free summers (Bégin et al., 2021; Michaud & Apollonio, 2022). The Svalbard lakes—Stuptjørna (Sval-STU), Jodavannet (Sval-JOD), and Heftyevatnet (Sval-HEF)—are surrounded by High Arctic tundra without any trees and with patchy vegetation concentrated around the lakes (Walker et al., 2005). The lakes in northern Sweden (Swe-BD03, Swe-BD11, and Swe-BD12) are in open mountain birch forest with extensive areas covered by heathland, scrubs, and tundra. Norwegian lakes Kulivatnet (Nor-KUL) and Fiskevatnet (Nor-FISK) are surrounded by a less sparse deciduous forest, with patches of peatlands and coniferous forest in the catchments (Dinerstein et al., 2017; Weiss & Banko, 2018). Currently, Norwegian lake Aspevatnet (Nor-ASP) is the only lake with an inflow of glacial meltwater. Both Nor-ASP and Sval-HEF are marine isolation lakes. Details on the location, physical parameters, climatic conditions, bedrock lithology, land cover, and presence of permafrost at each lake are given in Table 1.

2.2. Bathymetry, Sediment Core Collection, and Field Subsampling

To acquire lake morphometric properties, we conducted a bathymetric survey and calculated the dynamic ratio (DR) of each lake. This is a measure of the shape of the lake and its potential influence on water mixing and sediment interactions. In Sval-JOD and Sval-STU, we employed a Garmin ECHOMAP™ Plus 73SV with a CV52HW-TM transducer and a 5 Hz receiver to survey the bathymetry. Using a lead line, we mapped the bathymetry of Nor-DAL from lake ice at 29 locations. The bathymetry of Nor-ASP (Bakke et al., 2005), Nor-FISK (Paasche et al., 2004), Nor-KUL, and Swe-BD03, Swe-BD11, and Swe-BD12 (Klaus et al., 2021) was previously mapped (Figure 1). Depth soundings during coring were performed with a Hondex PS-7 Transducer. The lake DR was calculated as follows:

$$DR = \frac{\sqrt{a}}{D} \quad (1)$$

Figure 1. (a) Location of the study areas in Svalbard (b) and northern Scandinavia (c). The IBCAO base maps are modified after Jakobsson et al. (2012). (d) Aerial orthophotographs (©The Norwegian Polar Institute) of the catchments of Sval-JOD, Sval-STU, and Sval-HEF on Svalbard. Note that the bathymetry of Sval-STU is presented on a separate depth scale compared to the other lakes. (e) Aerial orthophotographs (©Statens Kartverk) of the catchments of Nor-ASP, Nor-KUL, Nor-FISK, and Nor-DAL in Troms, Norway. The scale bar for Nor-ASP is different from that of the other lakes. (f) Aerial orthophotographs (©Lantmäteriet) of the catchments of Swe-BD03, Swe-BD11, and Swe-BD12 in Abisko, Sweden. The bathymetry of each sampled lake, except for Sval-HEF, is presented.

Journal of Geophysical Research: Biogeosciences
10.1029/2024JG008508

Table 1
Physical Parameters of the Ten Studied Lakes

Lake code	Latitude (°N)	Longitude (°E)	Lake area (10^3 m^2)	Catchment area (10^3 m^2)	Max depth (m)	Mean depth (m)	Lake volume (10^3 m^3)	Lake dynamic ratio	Avg. Slope degree (°)	Elevation (m a.s.l.)	MAAT (°C)	MAP (mm)	Bedrock lithology	Landcover in catchment	Permafrost zones	Previous studies
Sval-HEF	77.9979	14.1486	15.1	148.1	6.5	3.3	49.1	0.04	11.2	43	−4.5	685	Mudstone/siltstone/ sandstone	P1. Prostrate dwarf-shrub, herb tundra	C	Kjellman et al. (2024), Farnsworth et al. (2022)
Sval-JOD	79.3382	16.0190	19.8	1,413.4	6.4	2.8	56.4	0.05	9.8	137	−7	300	Mica schist, metapsammite, amphibolite	P1. Prostrate dwarf-shrub, herb tundra	C	Kjellman et al. (2024), Voldstad et al. (2020)
Sval-STU	79.7019	15.9478	110.1	760.4	22.6	6.5	739.6	0.05	11.5	237	−7.5	600	Granitic gneiss, migmatite, amphibolite	B1. Cryptogam, herb barren	C	
Nor-KUL	69.7693	19.2761	41.2	244.8	6.3	2.3	93.2	0.09	10.0	87	5	875	Marble	Peat bogs	I	Balascio et al. (2018)
Nor-FISK	69.6531	19.8823	36.0	705.1	5.8	1.6	53.6	0.12	8.0	117	3	875	Quartzite	Peat bogs, broad-leaved forest	I	Paasche et al. (2004)
Nor-ASP	69.7502	19.9601	36.4	24,235.1	8.0	3.4	136.8	0.06	30.0	8	5	875	Phyllite + gabbro	Peat bogs, broadleaved forest, sparsely vegetated areas	S	Rasmussen et al. (2018), Bakke et al. (2005)
Nor-DAL	69.1906	20.7308	74.8	1,431.9	3.9	1.1	80.7	0.25	14.7	395	1	625	Arkose	Broadleaved forest, moors and heathland	I	McGowan et al. (2018), Nyman et al. (2008), Bjune et al. (2004)
Swe-BD03	68.4470	18.1303	81.5	1,666.1	8.1	2.0	163.8	0.14	12.5	496	−1	600	Granitoid, syenitoid, quartz monzodiorite and metamorphic equivalents	Moors and heathland	I	Olid et al. (2022)
Swe-BD11	68.4507	18.5741	56.1	1,961.2	8.7	3.3	182.7	0.07	8.7	399	−1	600	Granitoid, syenitoid, quartz monzodiorite and metamorphic equivalents	Moors and heathland	I	Olid et al. (2022)
Swe-BD12	68.4430	18.5777	18.1	78.0	6.0	1.4	24.9	0.10	7.8	420	−1	600	Granitoid, syenitoid, quartz monzodiorite, and metamorphic equivalents	Moors and heathland	I	Olid et al. (2022)

Note. The catchment area includes the lake area. The mean annual air temperature (MAAT) and mean annual precipitation (MAP) for the Svalbard lakes (1979–2014) are extracted from Østby et al. (2017). The MAAT and MAP for the Norwegian lakes (1991–2020) are from seNorge.no (2024), and for the Swedish lakes (1991–2020) from the Swedish Meteorological and Hydrological Institute (2024). The bedrock lithology for Svalbard is based on data from the Norwegian Polar Institute (2024), for Norway from the Geological Survey of Norway (2024), and for Sweden from the Geological Survey of Sweden (2024). The land cover in the catchments of Svalbard are from CAVM Team (2024), and CORINE Land Cover (2018) for Norway and Sweden. The permafrost zones are from Brown et al. (1997), whereas the catchment slope and elevation data are from the Terrengmodell Svalbard data set, provided by the Norwegian Polar Institute (2014) and the National Digital Elevation Model (Norwegian Mapping Authority, 2024), respectively. "Reference" column refers to catchment and lake data from other studies of the same lakes. The permafrost zones are categorized as follows: C, continuous; I, isolated; S, sporadic.

where a is the lake area (km^2) and $\underline{D}$ is the mean depth (m) (Håkanson, 1982). Measurements of dissolved oxygen, temperature, and specific conductivity in the water column were performed for Swe-BD11, Swe-BD12 (July 2021), and Nor-DAL (April 2021) using a multiparameter probe (Table S1 in Supporting Information S2).

Sediment cores were sampled to determine CH_4 concentration (Bulínová, 2025a), sediment porosity, and geochemical indicators for ecosystem productivity, which were acquired through spectral analysis. At each lake, two sediment cores were collected at the deepest point of the lake using a Universal surface corer (Aquatic Research Instruments) equipped with a 120 cm long coring tube with an inner diameter of 68 mm. Sediment cores were taken through a drilled hole in the lake ice in winter or through a hole in the bottom of a small zodiac in summer. The first sediment core was used for CH_4 and spectral analyses, and the second sediment core for porosity. From the first core, we collected multiple sub-samples (approximately 5 mL) by inserting a syringe (with the tip cut off) through 1-cm pre-drilled holes in the coring tubes. In the top 4–6 cm, samples were collected at 1-cm resolution, then every other cm until 28 cm, and every fourth cm from 28 to 60 cm. Below 60 cm, the sub-sample resolution was 5–10 cm depending on the length of the remaining core. Samples were divided into 4 mL for CH_4 (headspace gas) analysis and 1 mL for visible near-infrared reflectance spectroscopy (VNIRS). The sub-sample for headspace gas analysis was transferred to a 20 mL glass serum vial containing a glass bead and 5.00 mL of 1.0 M sodium hydroxide (NaOH), designed to terminate microbial activity. Each vial was immediately capped with a butyl/PTFE septum and an aluminum crimp seal, vigorously shaken to promote equilibration with the vial headspace, and stored at 4°C. Porosity (i.e., water content) was determined from the second sediment core by measuring the weight differences between wet and after freeze-dried samples. The total length of the organic sediments was measured by coring the entire postglacial sediment succession at each lake using a piston corer.

2.3. Sample Processing

2.3.1. Headspace CH_4 Gas Analysis

Concentrations of CH_4 ($[CH_4]$) in the headspace gas were determined using gas chromatography (*Thermo-Scientific*, Trace 1310, FID detector, MSieve 5A column) after injecting 10–25 µL of sample headspace with a gas-tight syringe into the instrument. The instrument's baseline noise level yielded a detection limit of approximately $1.5{\cdot}10^{-9}$ mmol. The sediment $[CH_4]$ was then calculated from the headspace gas concentration using the ideal gas law and further adjusted to account for the sample vial volume (Equation 2):

$$[CH_4] = \frac{pV}{RTV_{sed}} \quad (2)$$

where p represents pressure (Pa), V represents volume (L), R is the ideal gas constant (J mol^{-1} K^{-1}), T represents temperature (K), and V_{sed} is the volume of wet sediment (L). Analyses were conducted at The Arctic University (UiT) of Norway.

2.3.2. Visible and Near-Infrared Reflectance Spectroscopy (VNIRS)

To provide insight into lake color conditions, trophic status, and OC pools, we used VNIRS to infer both lake-water total OC (LW-TOC; mg TOC L^{-1}) concentrations at the time when a particular sediment layer was deposited and concentrations of chlorophyll *a* and related derivatives in the sediment (sedChl*a*; mg g^{-1}). The top 0–1 cm interval at each lake was analyzed, representing recent (~decadal) deposition. An important difference between these two values is that LW-TOC represents an integrated measure of the amount of TOC present in the lake-water column when the sediment sample was deposited (Meyer-Jacob et al., 2017), whereas the sedChl*a* represents the concentration of Chl*a* and its derivatives present in the actual sediment sample (Michelutti & Smol, 2016; Michelutti et al., 2005).

Before the spectroscopic analyses, sediment samples were freeze-dried and subsequently sieved (125 µm mesh) to remove the effects of water and particle size on the VNIRS signal (Meyer-Jacob et al., 2017). The VNIR spectra were recorded with a FOSS XDS Rapid Content Analyzer operated in diffuse reflectance mode at a wavelength range from 400 to 2,500 nm at Umeå University, Sweden. LW-TOC was inferred using the Partial Least Squares Regression (PLSR) calibration model described by Meyer-Jacob et al. (2017). This model was developed based on surface sediments and single measurements of LW-TOC taken during summer from 345 High Arctic to northern temperate lakes in Canada, Greenland, Sweden, and Finland. It covers a wide LW-TOC range

0.5–41 mg L^{-1}) encompassing expected values for our sampled lakes. The PLSR calibration has a cross-validated R^2 of 0.57 and a prediction error of 4.4 mg L^{-1}.

SedChl*a* concentration (i.e., Chlorophyll *a*, its derivatives, and their respective degradation products) was inferred using the pigment-based calibration model of Michelutti et al. (2005) based on the absorbance peak area between 650 and 700 nm. The model has a reported R^2 of 0.72 ($p < 0.05$) and an estimated lowest detection limit of 0.01 mg g^{-1}. SedChl*a* values in our sampled lakes were <0.06 mg g^{-1} (Table S1 in Supporting Information S2) that is, well within the calibration range (Michelutti et al., 2005).

2.4. CH_4 flux Modeling/Mass Transfer

We modeled the net production rates of CH_4 in various depth zones of the sediment profile and the diffusive CH_4 flux across the SWI. To compare differences in approaches on estimates, modeling of the flux was done using two of the main approaches for flux calculations: porewater modeling using the software PROFILE (Berg et al., 1998) and a mass transfer model. It is important to recognize several key assumptions and limitations of both approaches. They assume steady-state conditions (i.e., a constant concentration gradient and flux over time), one-dimensional vertical diffusion, and homogeneous sediment layers (as defined by input porosity and concentration data). Both approaches also rely on Fick's Law of diffusion. None of the approaches account for advective processes such as groundwater flow or bioturbation, which may influence CH_4 transport. The accuracy of the estimates is highly sensitive to input parameters, particularly porosity and concentration profiles.

The computer code PROFILE (Berg et al., 1998) is a widely used differential equation-solving software supported by statistical *F*-testing (e.g., Bartosiewicz et al., 2016; Clayer et al., 2018, 2020; D'Ambrosio & Harrison, 2022; Langenegger et al., 2019; Nordi et al., 2013; Rahalkar et al., 2009; Thottathil et al., 2022). PROFILE applies a one-dimensional diagenetic reaction-transport equation for solutes:

$$0 = \frac{d}{dx}\left(\varphi D_S \frac{d[CH_4]}{d_x}\right) + R_{net}^{CH_4} \quad (3)$$

In Equation 3, ϕ (%) represents the porosity, and Ds ($m^2\ s^{-1}$) is the effective diffusion coefficient of the CH_4 in sediments. The [CH_4] represents [CH_4] in (mM), whereas x represents the sediment depth (cm) (measured as positive downward from the SWI). The term R_{net}^{CH4} denotes the net production rate of CH_4 (or consumption rate if negative) (mmol m^{-3} day^{-1}). We used measured values of ϕ, [CH_4] profiles and D_s, which we assumed to be ϕD_w. Here, D_w represents the CH_4 tracer diffusion coefficient in water, and its value was $1.0158{\cdot}10^{-9}$ $m^2\ s^{-1}$ after correction assuming in situ temperature (4°C; from data in Jähne et al. (1987)). The [CH_4] at 0–1 cm of the sediment and at the deepest point of the measured concentration gradient served as boundary conditions. We then used the R_{net}^{CH4} values provided for various depth zones determined by the program. These values were obtained through a series of least-square fits to the measured concentration profile. The fits were compared using statistical *F*-tests to evaluate their accuracy. The program also provided an estimate of the diffusive CH_4 flux across the SWI, hereafter referred to as "PROFILE."

We also employed a mass transfer estimation of the diffusive CH_4 flux across the SWI, hereafter referred to as "mass transfer," using Fick's First Law (Equation 4):

$$F_{CH_4,diff} = -\varphi \frac{D_m}{\theta^2} \frac{dC_{CH_4}}{d_x} \quad (4)$$

where ϕ (%) is the measured porosity in the first cm of sediment, θ (dimensionless) is the tortuosity correction (we applied $\theta^2 = 1 - \ln(\phi)$) (Boudreau, 1997; Jähne et al., 1987), and D_m ($m^2\ s^{-1}$) stands for the molecular temperature-dependent diffusion of CH_4 in water, and is $1.02{\cdot}10^{-10}$ $m^2\ s^{-1}$. This coefficient was calculated for an assumed in situ temperature (4°C) from data in Jähne et al. (1987).

For the PROFILE and mass transfer approaches, we considered two sections of sediment profile. The first section is commonly used to measure the diffusive CH_4 flux across the SWI (Bartosiewicz et al., 2016; D'Ambrosio & Harrison, 2022; Langenegger et al., 2019). It involves a quasi-linear decrease of the concentration curve within the top few centimeters (typically 2–4 cm) of the sediment, determined by linear regression. This section is

referred to as "PROFILE: Top" or "mass transfer: Top." This quasi-linear decrease likely results from CH_4 diffusion and oxidation at the oxic-anoxic boundary. The second section extends from the SWI at the top to the main inflection point of the concentration curve at the bottom, where the increase is significantly reduced. This section is referred to as "PROFILE: Inflection" or "mass transfer: Inflection." Additionally, we used the entire measured sediment section in PROFILE only ("PROFILE: Long"). For depth zones of net CH_4 rates, we focused on the top 25 cm of the sediment, where most concentration profile changes occur.

2.5. Numerical Analyses

2.5.1. Multivariate Analyses

A Principal Component Analysis (PCA) was conducted on the 10 sampled lakes to explore and visually represent differences and similarities between the sampled lakes with regard to their landscape, morphometric and sediment parameters. We generated PCA biplots using the built-in R function prcomp (R Core Team, 2024), including the following variables (Figure S1): maximum lake depth, elevation, sedChl*a*, LW-TOC, DR, the total length of organic sediment, mean annual air temperature (MAAT), and catchment size. Prior to conducting the PCA, all variables except for MAAT were log-transformed, then variables were standardized by converting them to Z-scores (Mean = 0, Variance = 1).

2.5.2. Database Compilation of Diffusive CH_4 fluxes Across the SWI in Lakes

To provide a global context for our estimates of Arctic diffusive CH_4 flux across the SWI, and identify potential environmental predictors, we compiled a database of published diffusive CH_4 flux estimates across the SWI for 99 lakes worldwide, integrating published data with our estimates from the sampled lakes. Although this study focuses on lakes from high-latitude regions (north of ~60°N), the database encompasses a broad latitudinal range (2–79°N; Table S2 in Supporting Information S2; Bulínová, 2025b). There are 32 Arctic lakes (including the 10 lakes sampled for this study), 23 boreal lakes, 39 temperate lakes, and 5 lakes from the subtropics to tropics (Table S2 in Supporting Information S2). The synthesized estimates are derived from sediment diffusion modeling using Fick's first law ($n = 56$), sediment incubations ($n = 24$), hypolimnion or whole-lake budgets ($n = 18$), and benthic chamber sampling ($n = 1$). In addition to diffusive CH_4 flux estimates across the SWI, the data set includes basic morphometric, and biological data, such as lake surface area, maximum lake depth, and trophic status. Climate data including long-term (1970–2000) MAAT and mean annual precipitation were obtained from global 1-km gridded WorldClim 2 bioclimatic (BIO) variables (https://www.worldclim.org/data/index.html; Fick & Hijmans, 2017). Only natural lakes are included in the data set, and they encompass lake sizes from <0.01 km^2 to 32,900 km^2. The majority of observations in our data set are from lakes up to 0.5 km^2, with limited data available for larger lakes. Consequently, we selected this size category as it represents the most frequently observed group in our data set. In lakes where estimates were made for different locations within the lake, we report the estimate for the deepest location, and the average where multiple estimates for different points in time were taken (i.e., daily to seasonal).

2.5.3. Predictive Modeling of Diffusive CH_4 flux Across the SWI

We conducted predictive modeling to (a) identify the most important measured environmental variables driving diffusive CH_4 flux across the SWI for the 10 Arctic lakes sampled in this study (RF-sampled), and (b) identify variables that may be used as predictors across biomes for the expanded literature-based data set (RF-global). The *randomForest* package (version 4.7–1.1) (Liaw & Wiener, 2002) in R was used to build RF models that can capture complex non-linear relationships (see R script: Bulínová, 2025c). RF does not require dimensionality reduction prior to modeling and is robust to outliers and noise in the data due to the aggregation of multiple decision trees (Duan et al., 2023; Huang et al., 2022; Simon et al., 2023). The selected models were determined by selecting the "best" number of variables to use in each split (mtry) based on the minimum out-of-bag error. For each model, 66.6% of the observations were used for training and 33.3% were withheld for testing for cross-validation. The performance of the trained RF models was evaluated using R^2 values, and root-mean-squared error as performance metrics. To further analyze the RF-model results, we evaluated the importance of different variables and their partial dependence on the predicted diffusive CH_4 flux across the SWI. The importance of variables in the RF models was determined by calculating the mean decrease in accuracy.

Ultimately, we selected three RF models: (a) including the sampled lakes (RF-sampled), (b) small (<0.5 km^2) lakes from the database (RF-global (<0.5 km^2)), and (c) all lakes (RF-global (All)), respectively. The number of trees (*n_trees*) to try was set to 500, and the seed number was set to 71. The final selected parameters are *mtry* = 1, 1, and 1, and *n_trees* = 1, 45, and 130. For the RF-sampled model, a range of landscape, morphometric, hydrologic and ecosystem variables were tested (Table S3 in Supporting Information S2). After initial data exploration, we optimized model performance by carefully considering the variables to be removed from the analysis and prioritized easily measured variables. During this process, sedChl*a*, LW-TOC and maximum lake depth were selected for the final model. Multiple variables tested were highly correlated and many were therefore removed, such as Vegetation (most strongly correlated to LW-TOC; Table S4 in Supporting Information S2), mean lake depth (most strongly correlated to maximum lake depth) and the total length of organic sediment (inversely correlated to maximum lake depth). Porosity was excluded because it is used for flux calculation (Equations 3 and 4). As a target variable, we used the diffusive CH_4 flux across the SWI estimates obtained by mass transfer modeling when considering the top depth section of sediment only, which is commonly reported in the literature (e.g., D'Ambrosio et al., 2022; Langenegger et al., 2019; Lenstra et al., 2018; Rissanen et al., 2023), as opposed to those estimated using deeper intervals. After initial testing, seasonal and annual measurements were averaged in all models.

Due to the differences between the VNIRS-sediment inferred parameters (sedChl*a* and LW-TOC) and lake-water measurements of these variables, we excluded both of them from the database models (RF-global (All) and RF-global (<0.5 km^2)). We also excluded the DR, as it is not reported in many publications. Additionally, 24 lakes were removed because their diffusive CH_4 fluxes across the SWI were estimated via incubation experiments, whereas are focus was on *in situ* estimates. Five lakes were then removed as outliers due to their very large surface area (>2,000 km^2). Therefore, the final global data set used for RF-global (All) included 75 lakes, ranging in maximum depth from 1.5 to 1,450 m and lake surface area between 0.01 and 582 km^2. When considering only lakes with a surface area smaller than 0.5 km^2, the maximum lake depth ranged from 1.9 to 26 m. In this subset of lakes ($n = 41$), 16 measurements (or 6 when excluding this study) were from the Arctic, 7 measurements from the boreal region, and 18 from the temperate region.

3. Results

3.1. CH_4 Concentration Profiles

3.1.1. Variability in Sediment Porewater CH_4 Concentrations

Downcore [CH_4] profiles were systematically explored across the 10 sampled lakes (Figure 2). In general, the [CH_4] profiles show an initial steep increase with depth from the SWI down to 4–14 cm. After this initial steep increase, [CH_4] reaches an inflection point, marking a transition in the rate of change. Beyond this inflection point, [CH_4] stabilizes and remains relatively constant throughout the sediment profile. However, Sval-HEF stands out, showing a distinct [CH_4] decrease in the uppermost sediment layers. The between-lake variability in [CH_4] is large, even between lakes with similar porosity profiles (i.e., constant high porosity), such as Nor-KUL, Nor-FISK, Nor-DAL, Swe-BD11, and Swe-BD12 (Figure 2). Swe-BD11 displayed the lowest overall range of [CH_4] (0.02–0.2 mM) with a maximum concentration found at a depth of 52 cm, followed by glacial meltwater-fed Nor-ASP (0.01–0.5 mM; maximum at 36 cm) and Swe-BD03 (0.001–0.6 mM; maximum at 80 cm). In contrast, Nor-KUL exhibited the highest overall range of [CH_4] (0.61–2.8 mM) with a maximum at a depth of 32 cm, followed by Sval-JOD (0.05–1.9 mM; maximum at 84 cm) and Nor-DAL (0.39–1.8 mM; maximum at 24 cm). For the four lakes where [CH_4] profiles have been measured more than once (Nor-ASP, Nor-FISK, Nor-DAL, Nor-KUL), the visual comparison of profiles (Figure 2) suggests that the within-lake variability in [CH_4] is generally smaller than the between-lake variability, even when the measurements have been done in different seasons.

3.2. Modeled Net CH_4 Production Zones

The highest modeled net CH_4 production rate in each sediment profile ranged from 0.35 to 26 mmol m^{-3} day^{-1} and were generally associated with the top 10 cm of the sediment profile. The exception was Sval-HEF where the upper 10 cm were estimated to have negative net CH_4 production rates that is, consumption of CH_4 (Figure 3). The CH_4 modeling revealed two to five production zones within the vertical sediment profile in the lakes, labeled CH_4-Z_1, CH_4-Z_2, CH_4-Z_3, CH_4-Z_4 and CH_4-Z_5 from the SWI downward. Except for Nor-KUL and Sval-HEF, the

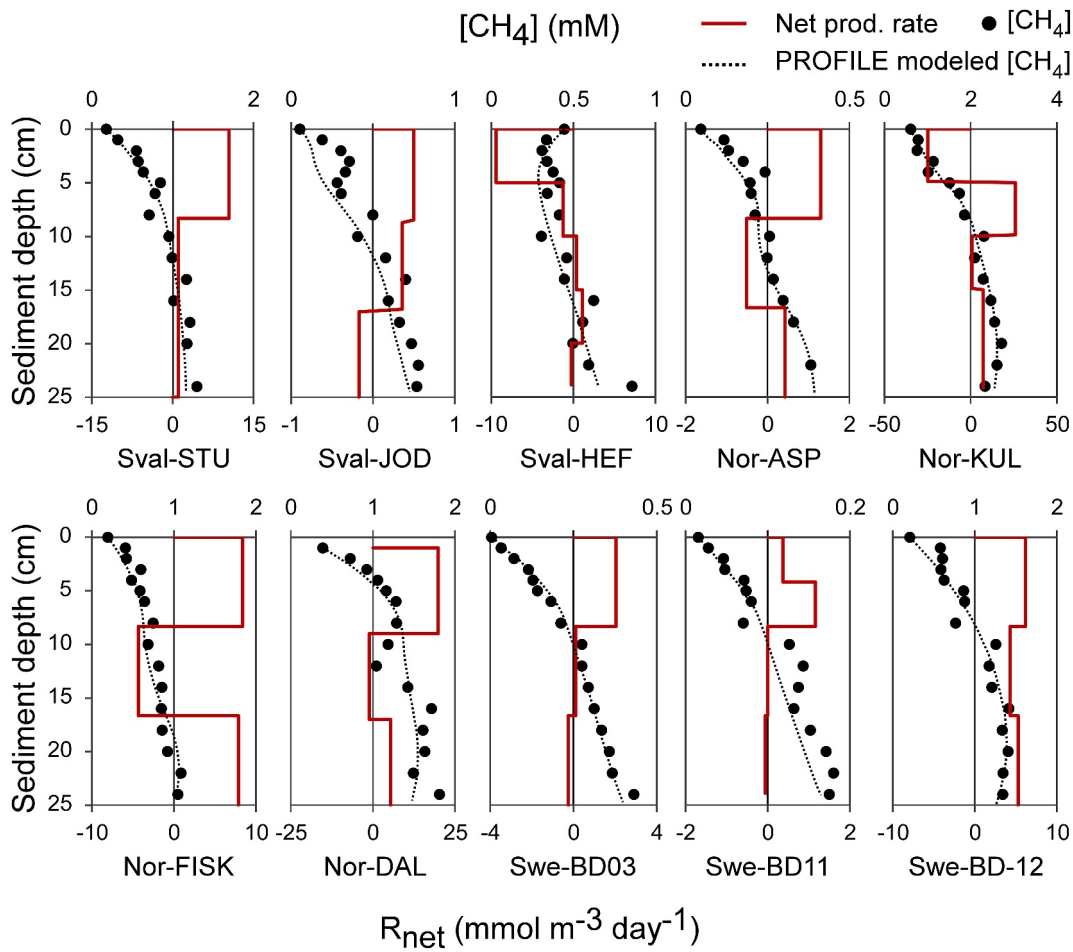

Figure 3. Comparison of the measured (black circles) and PROFILE-modeled (black dashed lines) concentration profiles of CH_4 in the sampled lakes. The red lines represent the net CH_4 reaction rate (R_{net}^{CH4}). Positive values represent production, negative values represent consumption. Across the 10 models evaluated, the Sum of Squared Errors ranged from $0.68 \cdot 10^{-6}$ to $9.60 \cdot 10^{-1}$. The R^2 ranged from 0.94 to 0.99.

first zone ("CH_4–Z_1") was represented by a steep increase in [CH_4], reaching down to 4–10 cm, and had the highest estimated net CH_4 production rates in the profile (Figure 3; Table S5 in Supporting Information S2). In Nor-KUL and Sval-HEF, the first production zone "CH_4-Z_1" was overlaid by a consumption zone, denoted as "CH_4-Z_0," where the net production rate was negative. Across all lakes, the CH_4-Z_1 was followed by zones with progressively lower net CH_4 production as we go down the profile (Figure 3). According to these estimates, most of the net CH_4 production occurred from 0 to as far down as 8 cm of the sediment, except lakes Nor-KUL and Swe-BD11 where the peak in net production is shifted deeper between 5 to 10 cm and 4–8 cm, respectively.

3.2.1. Diffusive CH_4 flux Across the SWI

We found that the highest positive flux estimates were obtained when using one of the "Top" interval approaches; however, there was no significant difference between the mass transfer and PROFILE approaches, nor between the intervals considered (Figure 4a; Table S7 in Supporting Information S2). The highest estimated top interval CH_4 fluxes were in Nor-ASP during winter (0.41 mmol m^{-2} day^{-1}), in Nor-DAL (3.1 mmol m^{-2} day^{-1}), Nor-KUL (2.7 mmol m^{-2} day^{-1}), Swe-BD03 (0.24 mmol m^{-2} day^{-1}), Swe-BD11 (0.74 mmol m^{-2} day^{-1}), Swe-BD12 (4.4 mmol m^{-2} day^{-1}), and Sval-STU (1.5 mmol m^{-2} day^{-1}) during summer, and in Nor-FISK in both seasons (2.6 mmol m^{-2} day^{-1} in winter and 1.1 mmol m^{-2} day^{-1} in summer). Sval-JOD (summer sampling), Sval-HEF, Nor-DAL, and Nor-KUL (all winter samplings) had the highest fluxes when considering the inflection section (0.18, 0.03, 2.9, and 1.5 mmol m^{-2} day^{-1}, respectively).

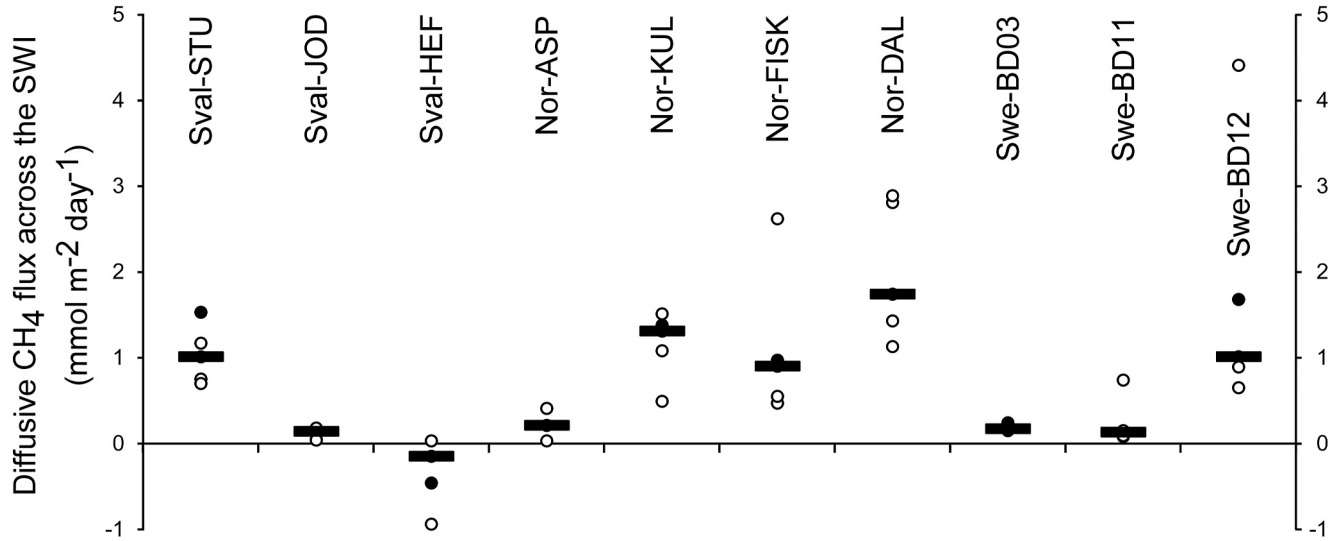

Figure 4. Comparison of five approaches to estimate diffusive CH_4 flux from sediments in the sampled lakes. The black circles represent "mass transfer: Top," the approach that we then selected for predictive modeling. The open symbols represent "mass transfer: Infl," "PROFILE: Top," "PROFILE: Infl," and "PROFILE: Long." Horizontal black lines represent median.

There was no significant sub-regional difference between the High Arctic and the Subarctic Scandinavian lakes (p-value = 0.62). In lakes where CH_4 fluxes were estimated on multiple occasions or during different seasons, there was substantial variability. The coefficient of variation for lakes Nor-ASP, Nor-KUL, Nor-FISK during different seasons was 100%, 45%, 10%, respectively, whilst for Nor-DAL, it was 39% between two winter samplings (Table S7 in Supporting Information S2).

The results also revealed that the between-lake variability in CH_4 diffusive flux estimates based on sediment data ranged from −5.0 to 4.4 mmol m^{-2} day^{-1} (median of 1.4 mmol m^{-2} day^{-1}) across all 10 sites, considering all the different estimation approaches (Figure 4a; Table S6 in Supporting Information S2). The largest inconsistency between approaches was observed in Nor-DAL during the winter sampling in 2021, where the different approaches yielded flux estimates between −5.0 and 3.1 mmol m^{-2} day^{-1}. This was followed by Nor-KUL (summer sampling; −3.1–2.7 mmol m^{-2} day^{-1}), and Swe-BD12 (summer sampling; 0.70–4.4 mmol m^{-2} day^{-1}). The most consistent values across the estimates were observed in Swe-BD03 (0.15–0.24 mmol m^{-2} day^{-1}) and Sval-JOD (0.04–0.18 mmol m^{-2} day^{-1}). For Nor-ASP and Nor-FISK, the winter sampling yielded higher fluxes.

3.2.2. Regional Variability in Diffusive CH_4 flux Across the SWI in Lakes

The CH_4 diffusive flux (modeled by "mass transfer: Top") values in the 10 sampled lakes (mean = 1.0 and median = 1.0 mmol m^{-2} day^{-1}) were similar when compared to other Arctic lakes smaller than 0.5 km^2 (n = 6; mean = 4.9 mmol m^{-2} day^{-1}, median = 4.1 mmol m^{-2} day^{-1}). The values for all Arctic lakes in the database (n = 18, including our data; mean = 2.2 mmol m^{-2} day^{-1}, median = 1.2 mmol m^{-2} day^{-1}) were comparable to estimates from boreal lakes (n = 13; mean = 1.9 mmol m^{-2} day^{-1}, median = 0.6 mmol m^{-2} day^{-1} Figure 5, Table S10 in Supporting Information S2). Estimates from both the Arctic and boreal lakes were significantly lower than those reported from temperate lakes of similar size (p-values <0.02; Figure 5; Table S8 in Supporting Information S2).

3.3. Statistical Analysis

3.3.1. Lake Grouping

The PCA showed two main groupings of the sampled Arctic lakes (further referred to as "high flux" and "low flux" lakes), defined based on their geochemical, limnological and landscape properties (Figure S1; Table 1; Figure 2). The "high flux" lakes (Nor-DAL, Nor-KUL, Nor-FISK, Swe-BD12, and Sval-STU) are shallower (3.9–6.3 m, except for Sval-STU at 22.6 m), located at lower latitude, and have higher sedChl*a*

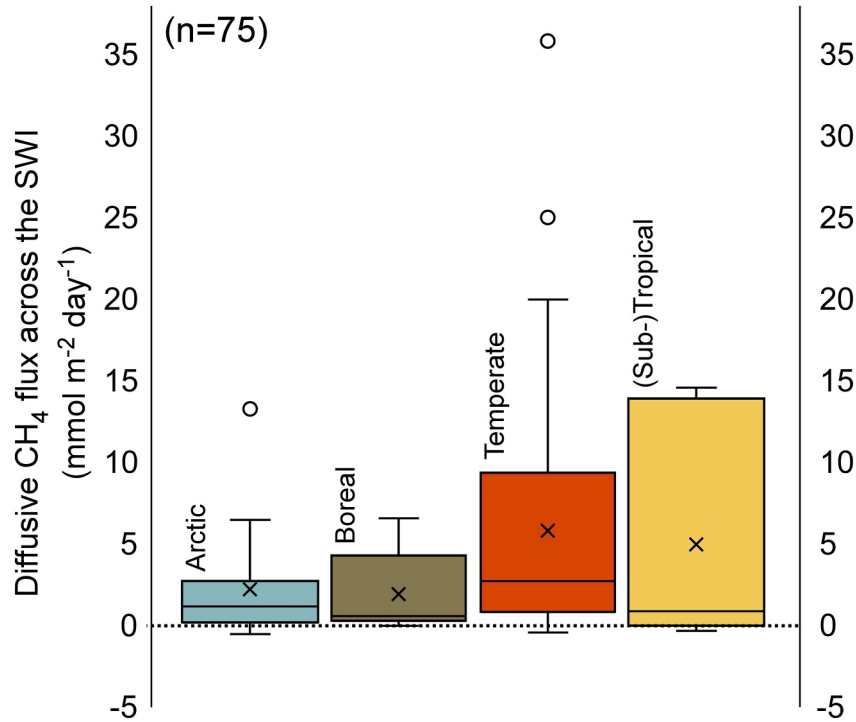

Figure 5. Diffusive CH_4 flux at sediment-water interface for all lakes in the database ($n = 75$). The Arctic group includes our 10 sampled lakes. The central box represents the interquartile range (IQR), calculated using the exclusive median method, with the lower and upper edges indicating the first and third quartiles, respectively. The horizontal line inside the box marks the median value. The whiskers extend to the smallest and largest values within 1.5 times the IQR from the quartiles. Circles denote outliers. The "X" symbol represents the mean value of the data.

(0.04–0.06 mg g^{-1}), a thicker OM sediment accumulation (2.6–4.1 m, except for Sval-STU with 1.0 m), a higher LW-TOC (8.0–15.6 mg L^{-1}, and Sval-STU 4.0 mg L^{-1}), and higher mean sediment porosity. This is in agreement with our CH_4-data, because the "high flux" lakes also had the highest sediment CH_4 concentrations, highest modeled CH_4 diffusive fluxes, and highest estimated net CH_4 production rates (Figure 3). Sval-STU also had a high [CH_4] and diffusive flux across the SWI, but due to its greater depth and low sedChl*a*, it is an outlier plotting most separate for this group. The "low flux" group (Sval-JOD, Sval-HEF, Swe-BD03, Swe-BD11, and Nor-ASP) is a more heterogeneous group in terms of latitude and catchment size, but the lakes are deeper (6.4–8.7 m) and consistently showed lower sedChl*a* values (0.01–0.04 mg g^{-1}), LW-TOC (<5.7 mg L^{-1}, except for Swe-BD11 at 12.7) total length of organic sediment (1.0–2.4 m) and lower mean porosity, suggesting low OM accumulation in sediments. According to our CH_4 data, lakes within this group had low [CH_4], low CH_4 fluxes across the SWI (<0.24 mmol m^{-2} day^{-1}) and net CH_4 production rates that did not exceed 2.6 mmol m^{-3} day^{-1}.

3.3.2. Random Forest—The Sampled Lakes

Random forest modeling showed that the most important environmental predictors of diffusive CH_4 flux across the SWI in the sampled lakes were VNIRS-Chl*a* (sedChl*a*) (10.3%), maximum depth (6.9%), and LW-TOC (5.3%) (Figure 6a). The percentage of variance explained was 39%, the mean of squared residuals was 0.2 and the average difference between the predicted and model estimates was 0.2 (log(mmol m^{-2} day^{-1})), which is well within the difference in flux estimate that may be attributed to the modeling approach selected, or the seasonal (or sampling) difference we were able to capture (Table S6 in Supporting Information S2). Generally, the diffusive CH_4 flux across the SWI increased with sedChl*a* and LW-TOC, and it decreased with lake depth (<10 m) except for the larger Svalbard lake Sval-STU (22.6 m; Figure 6).

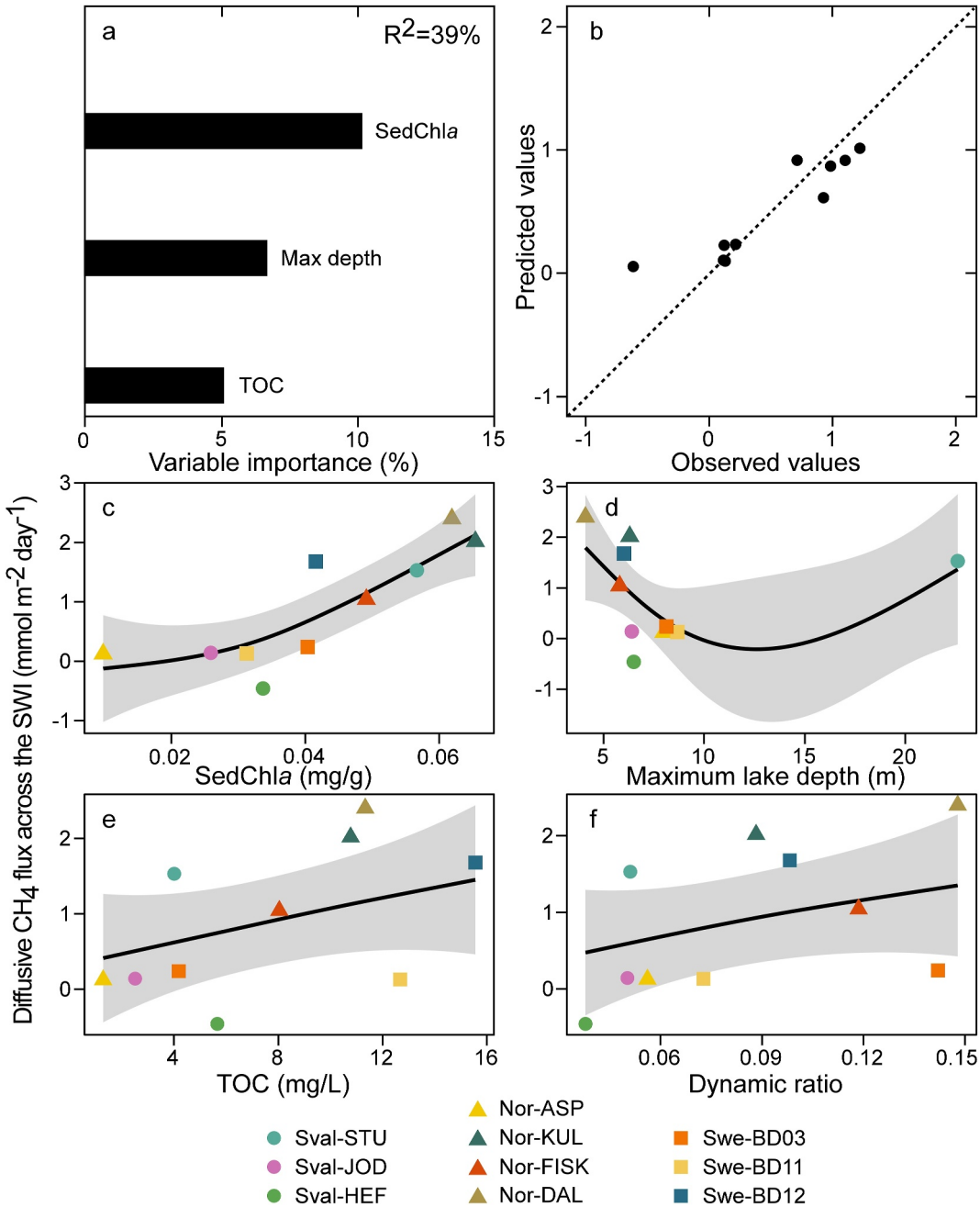

Figure 6. (a) Variables most important in predicting diffusive CH_4 flux across the sediment-water interface for the sampled lakes as evaluated by the random forest predictive model (RF-sampled). (b) RF-sampled predicted versus observed CH_4 diffusive flux (mmol m^{-2} day^{-1}) (in log scale). The red line represents the 1:1 line. (c) Diffusive CH_4 flux from the sampled lake sediments plotted against the predictor variables: sediment VNIRS-inferred chlorophyll *a* (sedChl*a*) ($p = 0.0027$). (d) Maximum lake depth ($p = 0.1228$). (e) LW-TOC ($p = 0.1661$). (f) Dynamic ratio ($p = 0.0490$). The significance of the interaction has been assessed by Spearman's rank correlation.

3.3.3. Random Forest—Global Database Lakes

When expanded to the global database of diffusive CH_4 flux across the SWI, the RF predictive model's performance decreased (Figure 7). When the larger lakes, but also a larger number of lakes were incorporated into the analysis (a) lakes <0.5 km^2, and (b) all database lakes), the percentage of variance explained changed to 45 and 26, respectively. The mean of squared residuals increased to 0.66 and 0.65 for these models, respectively, whereas

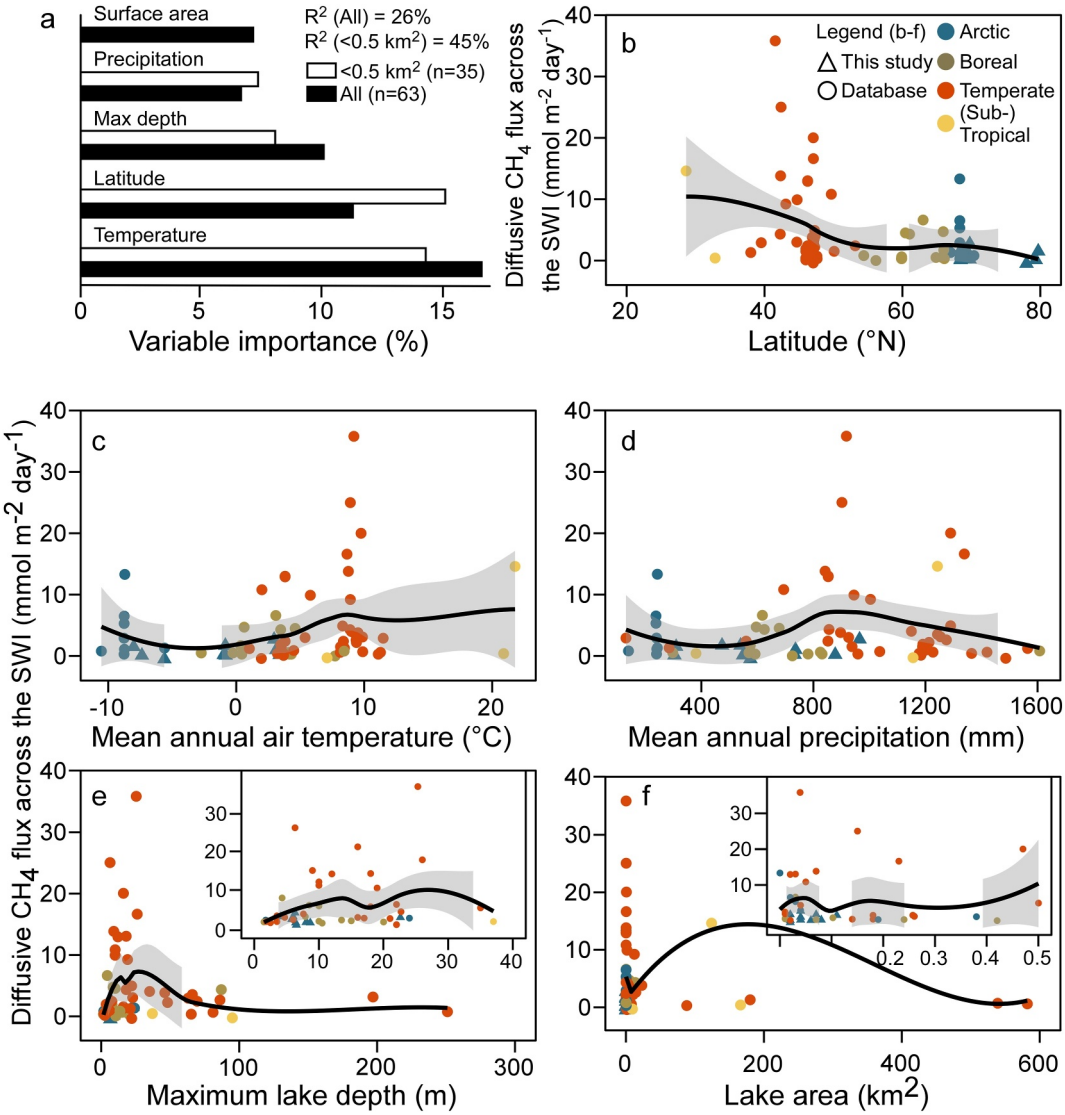

Figure 7. (a) Variables most important in predicting diffusive CH_4 flux across the sediment-water interface (SWI) for the database lakes including lakes with area <0.5 km^2 (RF-global (<0.5 km^2)), and all lakes in the database (RF-global (All)). (b) Diffusive CH_4 flux across the SWI from the compiled database lake sediments plotted against (selected) predictor variables: Latitude ($p = 0.0146$). (c) Annual mean air temperature ($p = 0.0298$). (d) Annual precipitation ($p = 0.5909$), (e) Maximum lake depth ($p = 0.2015$). (f) Lake surface area ($p = 0.8628$). The significance of the interaction has been assessed by Spearman's rank correlation. Inset graphs in panels (e) and (f) are zoomed in to show lakes with maximum lake depth <40 m and lakes with surface area <0.5 km^2. The mean of squared residuals are 0.66 and 0.65, and the root mean squared error is 0.78 and 0.79 log(mmol m^{-2} day^{-1}) for the RF-global (<0.5 km^2) and (RF-global (All)), respectively.

the average difference between the predicted and model estimates increased to 0.77 and 0.79 (log (mmol m^{-2} day^{-1}). The RF predictive modeling showed that the most important environmental predictors of diffusive CH_4 flux from the sediment were MAAT (14.2%, and 16.5%), latitude (15%, and 11.2%), maximum depth (8%, and 10%), annual precipitation (7.3%, and 6.6%), and lake surface area (only included in RF-global (All), 7.1%; Figure 7a). Significant linear relationships over the full gradient were found for latitude ($p < 0.05$) and MAAT ($p < 0.1$) where the diffusive CH_4 flux generally increased southward and with increasing mean air temperature.

4. Discussion

4.1. Variability of CH_4 Diffusive Flux Across the SWI

Our porewater modeling suggests a positive net exchange of CH_4 across the SWI—that is, that CH_4 leaves the sediment—in nine of the sampled lakes (0.1–4.4 mmol m^{-2} day^{-1}). The exception was Sval-HEF, where the net exchange across the SWI was negative (−0.5 mmol m^{-2} day^{-1}; Figure 4, Table S6 in Supporting Information S2). The sampled lakes exhibit similar CH_4 fluxes across the SWI (median = 0.6 mmol m^{-2} day^{-1}; Table S10 in Supporting Information S2) compared to those reported in the database for six other Arctic lakes of similar size (<0.5 km^2) (median = 4.1 mmol m^{-2} day^{-1}; Table S10 in Supporting Information S2). The range of estimates for the CH_4 diffusive flux across the SWI in the sampled lakes is also within reported flux estimates from boreal lakes of similar size (<0.5 km^2), but with greater range of values (mean = 1.3 mmol m^{-2} day^{-1}, range = 0.3–6.6 mmol m^{-2} day^{-1}; Figure 5). Arctic and boreal lakes exhibit, however, a significantly lower diffusive CH_4 flux across the SWI than temperate lakes ($p < 0.05$ and 0.01 when compared with Arctic and boreal lakes, respectively; Table S8 in Supporting Information S2). Consistent with this result, variables associated with enhanced ecosystem productivity, such as warmer (higher MAAT, lower latitude) and wetter (higher annual precipitation) conditions, were identified as the most important predictors in the RF-global (All) models (Figure 7; Table S9 in Supporting Information S2). Our results suggest that a shift toward warmer conditions, which enhances ecosystem productivity at high latitudes, would increase CH_4 production in lakes, with likely consequences on the contribution by northern lakes on global CH_4 budget expected for the future (Wik et al., 2016).

The three sampled High Arctic lakes (Sval-HEF, Sval-JOD, and Sval-STU) showed some of the highest ranges of values in flux estimates. This variability also goes beyond the seasonal/interannual variability we measured in the Subarctic lakes, which was not found to be an important predictor variable of CH_4 flux (Table S6 in Supporting Information S2; Figure 6). The potential influence of for example, lake mixing regime on lake bottom redox conditions affecting CH_4 flux (Vachon et al., 2019) may not be captured by the relatively limited sampled lake number and temporal resolution (Natchimuthu et al., 2016), at least beyond the effect of multiple sampling attempts at somewhat different locations between years/seasons. Only one lake (Sval-HEF) had sediments that consumed more CH_4 than was produced (Figure 4, Table S6 in Supporting Information S2), suggesting higher production may occur in the water column or, more likely, deeper in the sediments, as well as some level of methane oxidation. Although the deeper sediment production is supported by "PROFILE: Long" (0.03 mmol m^{-2} day^{-1}) and "mass transfer: Inflection' (0.03 mmol m^{-2} day^{-1}) (Table S6 in Supporting Information S2), a deep geogenic origin of the CH_4 may also explain this outlier, particularly considering the presence of bituminous mudstone in this catchment, which has been associated with CH_4 emissions on Svalbard (Birchall et al., 2023). Although we had expected that High Arctic lakes might stand out given the relatively low productivity of these systems, their [CH_4] profiles and fluxes were within the range of the Subarctic lakes from our study. This high variability suggests that not only ecosystem productivity along climatic gradients but also other factors are driving CH_4 production.

The variability in CH_4 diffusive flux across the SWI in these Arctic lakes may also at least partly be attributed to differences in porosity. Most lakes in this study display consistently high porosity throughout their profile, except for Sval-JOD, Sval-HEF, and Nor-ASP. Overall, lakes categorized within the "high flux" group demonstrate higher porosity within their sediments (Figure S1). In the case of Sval-JOD, there is a 15–20-cm-thick silty fine sand layer capping the deeper sediments (see unit L4 in Figure S1 in Kjellman et al., 2024), leading to a buildup of CH_4. In the case of Sval-HEF, the upper sediments are more permeable than the deeper layers, which presumably leads to less build-up of CH_4 in the upper part. Nor-ASP has an overall low porosity of 0.3–0.7 (except the top 2 cm), with a thin layer with very low porosity at 8–10 cm. However, unlike for Sval-JOD, the measured CH_4-profiles in Nor-ASP did not indicate any buildup of CH_4 in deeper sediment. This indicates that the low porosity layer is not thick enough to prevent diffusion.

The new data we provide on diffusive fluxes across the SWI in Arctic lakes further support the importance of consistent methodologies for estimating and, eventually, upscaling (D'Ambrosio & Harrison, 2022). Our different approaches to estimate diffusive flux across the SWI highlight that although general trends between lakes could be reproduced using multiple approaches, the differences between approaches were at times as high as between-lake differences (Figure 4, Table S6 in Supporting Information S2). Even though expanding CH_4 measurements into deeper sediments resulted in higher CH_4 estimates at some lakes (Nor-DAL, Nor-KUL, and Sval-JOD), we found no systematic direction of this variability, neither between the approaches of flux modeling

nor down-core. However, we provide evidence that because most studies estimate flux based on shallow sediments, significant CH_4 production in deeper sediments in some systems might have been overlooked. For instance, a negative production rate may be explained at Sval-HEF when taking into account the estimates from 14 cm (flux rate = 0.03 mmol m^{-2} day^{-1}), showing that CH_4 in the top sediments is likely produced—or originates—deeper down. CH_4 production in deep sediments is usually associated with highly organic-rich sediments or sediments in highly acidic or basic lakes where CH_4 production in surface sediments is inhibited (D'Ambrosio & Harrison, 2022). At the sampled lakes, the total length of organic sediment was an important factor separating the "high flux" from the "low-flux" lakes (Figure S1). Overall, our results highlight that beyond the difference in approach, significant regional (i.e., within the Arctic) variability in CH_4 diffusive fluxes was identified.

4.2. Lake Primary Production as the Main Control of CH_4 Production and Diffusive Flux in Arctic Lakes and Additional Drivers of Landscape Variability

4.2.1. Autochthonous Organic Matter Fuels Diffusion of CH_4 Across the SWI in Small Arctic Lakes

The modeling estimates indicate that the bulk of CH_4 that leaves the sediment through the SWI originated from the upper 10 cm (Figure 3). This suggests that it is the recently deposited OM that fuels sediment CH_4 diffusive flux across the SWI in those lakes. This is consistent with sediment incubations from a range of lakes showing that OM in the sediment controls the production and flux of CH_4 across the SWI (Grasset et al., 2018, 2021; Isidorova et al., 2019; Moras et al., 2024; Schwarz et al., 2008; West et al., 2012, 2015). Furthermore, algal OM, represented by sedChl*a*, emerged as the strongest predictor of diffusive CH_4 flux across the SWI in the RF-sampled model, with fluxes becoming larger with increasing sedChl*a* (Figure 6c). Even though sedChl*a* is a measure both of the chlorophyll pigments and their degradation products and hence does not only reflect fresh algal-OM, it provides a measure of quantity and quality of the algal OM. As expected, given the strong link between DOC and PP in northern lakes (Karlsson et al., 2009; Seekell et al., 2015; Solomon et al., 2013), LW-TOC was also identified as a positive predictor in the RF-sampled model (Figure 6). The CH_4 flux and both spectrally derived variables were significantly correlated to other environmental indicators of enhanced ecosystem productivity—higher vegetation cover, less extensive permafrost, and thicker OM sediment accumulation (Table S4 in Supporting Information S2). In relatively clear and shallow lakes, where the light is sufficient for photosynthesis throughout the water column, a positive correlation between DOC and PP has been explained by input of DOC-associated nutrients and by DOC promoting elevated levels of CO_2 (Jansson et al., 2012). Our analyses, therefore, point to high-quality autochthonous substrate availability being critical to CH_4 diffusion across the SWI in small Arctic lakes. The increased PP, transport, and deposition of autochthonous OC fuel CH_4 production, thereby enhancing CH_4 diffusion from sediments in these oligotrophic, relatively clear-water Arctic lakes.

4.2.2. Mechanisms of CH_4 Production in Arctic Lake Sediments

Svalbard lake Sval-STU stood as an outlier in our "high flux" lakes group, particularly due to its location in the high Arctic, with high porosity compared to other sampled Svalbard lakes, and deep basin (>22 m). The lake sits at high elevation, and often remains covered by ice for long periods, with only a small ice-free area in the peak of summer. Due to its deep basin, the bottom of the lake is unlikely to become oxidized, leading to the main process of OM reduction being the production of CH_4. We therefore propose that the high flux (1.5 mmol m^{-2} day^{-1}) estimated at this lake is likely due to the otherwise limited mineralization of OM (besides methanogenesis).

Our porewater modeling also indicates that CH_4 consumption within the CH_4-Z_0 sediments may have been more important at lakes Nor-KUL, Sval-JOD and Sval-HEF, which show low net CH_4 production rates (−24.88 to 0.52 mmol m^{-3} day^{-1}; Figure 3). Lake Sval-HEF showed one of the most notable rates of CH_4 loss (−9.42 mmol m^{-3} day^{-1}; Figures 4 and 5) and was one of few lakes in the database with a negative flux (Table S2 in Supporting Information S2). A possible explanation for the increased CH_4 consumption in the Sval-HEF sediments could be the presence of alternative electron acceptors that would allow for fermentation and methanotrophy in the zone of CH_4 consumption (0–5 cm; Figure 3). Even though we assume there is no aerobic CH_4 oxidation in deep sediments, anaerobic oxidation of CH_4 (AOM) has been detected at the top as well as deeper in Arctic lake sediments elsewhere. In the sediments of Arctic Lake Doughnut, AOM was estimated to 12%–30% of the CH_4 produced, with the highest rate observed in the top 2.5 cm (Martinez-Cruz et al., 2018). AOM occurs under anoxic conditions in the presence of alternative electron acceptors (such as sulfates, nitrates, iron,

manganese, and humic substances) and can significantly constrain CH_4 emissions to the atmosphere. Measurements of CH_4 stable isotopes would help establish whether the origin of CH_4 at Sval-HEF might be biogenic or rather geogenic, with potentially a strong role of AOM (Whiticar, 1996; Whiticar & Faber, 1986). Overall, the direction of net CH_4 production was variable between lakes and down-core, suggesting that other processes (e.g., different methanogenic pathways, different importance of OM mineralization) result in regional upscaling uncertainties that may not be well accounted for in global modeling efforts.

4.2.3. Intertwined Arctic Landscape and Climate Controls

Though our study shows that ecosystem productivity has a major impact on CH_4 diffusive fluxes in the 10 sampled Arctic lakes, we also found high variability that we attribute to landscape and climate controls. Specifically, lower maximum depth was the most important morphometric predictor of greater flux for the 10 sampled lakes, whereas higher DR was also significantly correlated with the flux, although it was not included in the final selected model (Figure 6a). Our "high flux" lakes are indeed shallower and have higher DR ("high flux" median = 0.10; "low flux" median = 0.06; Figure 7). When the maximum depth increases, the importance of the shape of the lake basin becomes more apparent, especially for processes such as the redistribution of carbon (e.g., sediment focusing), lake stratification, oxygen regime, or carbon accumulation (Boehrer & Schultze, 2008). In contrast, higher lake-water temperatures may be expected in smaller water volumes with relatively larger shallow zones (higher DR, Table 1), thus promoting PP. This is consistent with shallow lakes showing higher sedChl*a*, higher LW-TOC, and higher OC accumulation (Figure 6). The interplay between lake depth and surface area can also impact oxygen levels and CH_4 production through thermal stratification and mixing (Fee et al., 1996; Holgerson & Raymond, 2016). This effect may play a role in the sampled small Arctic lakes but becomes more important where a larger range for those variables is considered (Figure 7). As the database models suggest, morphometric and climate variables reliably account for important drivers of diffusive CH_4 flux that may be related to OM production and preservation in small lakes. However, we clearly lack critical information for accurately predicting fluxes in larger lakes, such as hydrological connectivity, lake shape and the spatial variability of fluxes within such large lakes (Figure 7a). Furthermore, it is evident from our database that fluxes have only been quantified in relatively few large lakes, particularly at higher latitudes, thus limiting the scope of our global training data set for predictions. The highly variable sediment diffusive CH_4 emissions from Arctic lakes reported in this study stress the importance of accurately representing the variability in lake types for global upscaling estimates and future predictions.

5. Conclusions

We estimated diffusive fluxes of CH_4 across the SWI in 10 lakes in Subarctic Scandinavia and High Arctic Svalbard. The estimated fluxes ranged from −0.46 to 3.1 mmol m^{-2} day^{-1}, which is comparable to fluxes observed in other Arctic and boreal lakes, but lower than for temperate and tropical lakes. Although we show that CH_4 production was contained within the top ∼10 cm of the sediments in most of those Arctic lakes, we strongly recommend measuring at least 20 cm of sediment depth to be able to explore potentially higher CH_4 production in deeper sediments. Our RF predictive modeling indicates that Arctic between-lake variability is primarily associated with autochthonous PP of organic carbon, as well as factors favoring the deposition of OM in sediments. We found that morphometric and landscape variables, including lake depth and lake surface area, as well as climatic factors such as warmer and wetter conditions enhancing ecosystem productivity have a significant impact on the diffusive CH_4 flux across the SWI and across biomes. By expanding the sampled lake types and linking the diffusive CH_4 flux across the SWI to climatic and landscape variables, we provide insights necessary for the evaluation of process-based CH_4 dynamical models.

Data Availability Statement

The Lake Sediment Methane Diffusive Flux Database (1.0.0) compiled for this study is available at Zenodo via https://doi.org/10.5281/zenodo.15683902 under a Creative Commons Attribution license (Bulínová, 2025b).

The Methane in sediments of small Arctic lakes (1.0.0) data set used in this study is preserved at Zenodo and can be accessed via https://doi.org/10.5281/zenodo.15683559 under a Creative Commons Attribution license (Bulínová, 2025a).

The Random Forest modeling script used for methane flux analysis is preserved at Zenodo. Version 1 of the script is available at https://doi.org/10.5281/zenodo.15678563 under a Creative Commons Attribution license (Bulínová, 2025c). The script is also available on GitHub at https://github.com/MariBulin/RandomForest_methane-flux.

Acknowledgments
We acknowledge funding for the PolarCH_4ives project from the Research Council of Norway (Grant 294929). For additional funding, we thank the Research Council of Norway for Arctic Field Grants to MB and AR (Grants 322301 and 342064), Carl Trygger Stiftelse to AR, the Trond Mohn Research Foundation (TMF) for supporting WGMvdB, and fieldwork with Grant TMS2021STG01, the Nansen Foundation to MB, and Erasmus+ to MB. The Swedish Polar Research Secretariat and SITES are acknowledged for supporting our work at the Abisko Scientific Research Station. The University Centre in Svalbard (UNIS) is thanked for supporting parts of the fieldwork on Svalbard. Nicholas Balascio and Scott Anderson kindly shared bathymetry data from Kulivatnet. Michael Retelle, Joseph Buckby, Matteus Lindgren, Claudio Argentino, Carmen Braun, Andreas Grumstad, Sara Andersson, Kaj Lynøe, Oldřich Kaucký, Matteusz Strzelecki, and Sebastian Lindhorst kindly assisted during fieldwork; and Lyngen Lodge Tour Guides provided logistical assistance. We thank Jan Karlsson, Matteus Lindgren, and Maarten van Hardenbroek van Ammerstol for their valuable advice and discussions. Two anonymous reviewers are thanked for constructive suggestions for improvement of the manuscript.

References

Aben, R. C. H., Barros, N., Van Donk, E., Frenken, T., Hilt, S., Kazanjian, G., et al. (2017). Cross continental increase in methane ebullition under climate change. *Nature Communications*, *8*(1), 1–8. https://doi.org/10.1038/s41467-017-01535-y

Bakke, J., Dahl, S. O., & Nesje, A. (2005). Lateglacial and early Holocene palaeoclimatic reconstruction based on glacier fluctuations and equilibrium-line altitudes at northern Folgefonna, Hardanger, western Norway. *Journal of Quaternary Science*, *20*(2), 179–198. https://doi.org/10.1002/jqs.893

Balascio, N. L., D'Andrea, W. J., Anderson, R. S., & Wickler, S. (2018). Influence of vegetation type on n-alkane composition and hydrogen isotope values from a high latitude ombrotrophic bog. *Organic Geochemistry*, *121*, 48–57. https://doi.org/10.1016/j.orggeochem.2018.03.008

Bartosiewicz, M., Laurion, I., Clayer, F., & Maranger, R. (2016). Heat-wave effects on oxygen, nutrients, and phytoplankton can alter global warming potential of gases emitted from a small shallow lake. *Environmental Science and Technology*, *50*(12), 6267–6275. https://doi.org/10.1021/acs.est.5b06312

Bastviken, D., Ejlertsson, J., Sundh, I., & Tranvik, L. (2003). Methane as a source of carbon and energy for lake pelagic food webs. *Ecology*, *84*(4), 969–981. https://doi.org/10.1890/0012-9658(2003)084[0969:maasoc]2.0.co;2

Bégin, P. N., Tanabe, Y., Rautio, M., Wauthy, M., Laurion, I., Uchida, M., et al. (2021). Water column gradients beneath the summer ice of a High Arctic freshwater lake as indicators of sensitivity to climate change. *Scientific Reports*, *11*(1), 1–12. https://doi.org/10.1038/s41598-021-82234-z

Berg, P., Risgaard-Petersen, N., & Rysgaard, S. (1998). Interpretation of measured concentration profiles in sediment pore water. *Limnology & Oceanography*, *43*(7), 1500–1510. https://doi.org/10.4319/lo.1998.43.7.1500

Birchall, T., Jochmann, M., Betlem, P., Senger, K., Hodson, A., & Olaussen, S. (2023). Permafrost trapped natural gas in Svalbard, Norway. *Frontiers in Earth Science*, *11*(December), 2–4. https://doi.org/10.3389/feart.2023.1277027

Bjune, A. E., Birks, H. J. B., & Seppä, H. (2004). Holocene vegetation and climate history on a continental-oceanic transect in northern Fennoscandia based on pollen and plant macrofossils. *Boreas*, *33*(3), 211–223. https://doi.org/10.1080/03009480410001244

Bodmer, P., Wilkinson, J., & Lorke, A. (2020). Sediment properties drive spatial variability of potential methane production and oxidation in small streams. *Journal of Geophysical Research: Biogeosciences*, *125*(1), e2019JG005213. https://doi.org/10.1029/2019JG005213

Boehrer, B., & Schultze, M. (2008). Stratification of lakes. *Reviews of Geophysics*, *46*(2), RG2005. https://doi.org/10.1029/2006rg000210

Boudreau, B. P. (1997). *Diagenetic models and their implementation* (Vol. 505, p. 132). Springer. https://doi.org/10.1007/97S-3-642-60421-S

Bretz, K. A., & Whalen, S. C. (2014). Methane cycling dynamics in sediments of Alaskan Arctic Foothill lakes. *Inland Waters*, *4*(1), 65–78. https://doi.org/10.5268/iw-4.1.637

Brown, J., Ferrians, O. J., Jr., Heginbottom, J. A., & Melnikov, E. S. (1997). *Circum-Arctic map of permafrost and ground-ice conditions (Circum-Pacific Map No. 45)*. U.S. Geological Survey. https://doi.org/10.3133/cp45

Bulínová, M. (2025a). Lake sediment methane diffusive flux database (1.0.0) [Dataset]. *Zenodo*. https://doi.org/10.5281/zenodo.15683902

Bulínová, M. (2025b). MariBulin/RandomForest_methane-flux: RandomForest_methane-flux (version 1). *Zenodo*. https://doi.org/10.5281/zenodo.15678563

Bulínová, M. (2025c). Methane in sediments of small Arctic lakes (1.0.0) [Dataset]. *Zenodo*. https://doi.org/10.5281/zenodo.15683559

Carnevali, P. B. M., Rohrssen, M., Williams, M. R., Michaud, A. B., Adams, H., Berisford, D., et al. (2015). Methane sources in arctic thermokarst lake sediments on the N orth S lope of A laska. *Geobiology*, *13*(2), 181–197. https://doi.org/10.1111/gbi.12124

CAVM Team. (2024). Raster circumpolar arctic vegetation map (scale 1:7,000,000). In *Conservation of arctic Flora and Fauna, Akureyri, Iceland.*

Clayer, F., Gélinas, Y., Tessier, A., & Gobeil, C. (2020). Mineralization of organic matter in boreal lake sediments: Rates, pathways, and nature of the fermenting substrates. *Biogeosciences*, *17*(18), 4571–4589. https://doi.org/10.5194/bg-17-4571-2020

Clayer, F., Moritz, A., Gélinas, Y., Tessier, A., & Gobeil, C. (2018). Modeling the carbon isotope signatures of methane and dissolved inorganic carbon to unravel mineralization pathways in boreal lake sediments. *Geochimica et Cosmochimica Acta*, *229*, 36–52. https://doi.org/10.1016/j.gca.2018.02.012

CORINE Land Cover. (2018). CORINE land cover 2018 (raster 100 m). https://doi.org/10.2909/960998c1-1870-4e82-8051-6485205ebbac

Cunada, C. L., Lesack, L. F. W., & Tank, S. E. (2018). Seasonal dynamics of dissolved methane in lakes of the Mackenzie Delta and the role of carbon substrate quality. *Journal of Geophysical Research: Biogeosciences*, *123*(2), 591–609. https://doi.org/10.1002/2017jg004047

D'Ambrosio, S. L., & Harrison, J. A. (2021). Methanogenesis exceeds CH_4 consumption in eutrophic lake sediments. *Limnology And Oceanography Letters*, *6*(4), 173–181. https://doi.org/10.1002/lol2.10192

D'Ambrosio, S. L., & Harrison, J. A. (2022). Measuring CH_4 fluxes from lake and reservoir sediments: Methodologies and needs. *Frontiers in Environmental Science*, *10*(March), 1–19. https://doi.org/10.3389/fenvs.2022.850070

D'Ambrosio, S. L., Henderson, S. M., Nielson, J. R., & Harrison, J. A. (2022). In situ flux estimates reveal large variations in methane flux across the bottom boundary layer of a eutrophic lake. *Limnology & Oceanography*, *67*(10), 2119–2139. https://doi.org/10.1002/lno.12193

de Jong, A. E., in't Zandt, M. H., Meisel, O. H., Jetten, M. S., Dean, J. F., Rasigraf, O., & Welte, C. U. (2018). Increases in temperature and nutrient availability positively affect methane-cycling microorganisms in Arctic thermokarst lake sediments. *Environmental Microbiology*, *20*(12), 4314–4327. https://doi.org/10.1111/1462-2920.14345

DelSontro, T., Beaulieu, J. J., & Downing, J. A. (2018). Greenhouse gas emissions from lakes and impoundments: Upscaling in the face of global change. *Limnology and Oceanography Letters*, *3*(3), 64–75. https://doi.org/10.1002/lol2.10073

Dinerstein, E., Olson, D., Joshi, A., Vynne, C., Burgess, N. D., Wikramanayake, E., et al. (2017). An Ecoregion-based approach to Protecting Half the terrestrial Realm. *BioScience*, *67*(6), 534–545. https://doi.org/10.1093/biosci/bix014

Downing, J. A., Prairie, Y. T., Cole, J. J., Duarte, C. M., Tranvik, L. J., Striegl, R. G., et al. (2006). Abundance and size distribution of lakes, ponds and impoundments. *Limnology & Oceanography*, *51*(5), 2388–2397. https://doi.org/10.1016/B978-012370626-3.00025-9

Duan, H., Xiao, Q., Qi, T., Hu, C., Zhang, M., Shen, M., et al. (2023). Quantification of diffusive methane emissions from a large eutrophic lake with Satellite Imagery. *Environmental Science and Technology*, *57*(36), 13520–13529. https://doi.org/10.1021/acs.est.3c05631

Duc, N. T., Crill, P., & Bastviken, D. (2010). Implications of temperature and sediment characteristics on methane formation and oxidation in lake sediments. *Biogeochemistry*, *100*(1), 185–196. https://doi.org/10.1007/s10533-010-9415-8

Farnsworth, W. R., Ingólfsson, Ó., Mannerfelt, E. S., Kalliokoski, M. H., Guðmundsdóttir, E. R., Retelle, M., et al. (2022). Vedde Ash constrains Younger Dryas glacier re-advance and rapid glacio-isostatic rebound on Svalbard. *Quaternary Science Advances*, *5*(June 2021), 100041. https://doi.org/10.1016/j.qsa.2021.100041

Fee, E. J., Hecky, R. E., Kasian, S. E. M., & Cruikshank, D. R. (1996). Physical and chemical responses of lakes and streams. *Limnology & Oceanography*, *41*(5), 912–920.

Fick, S. E., & Hijmans, R. J. (2017). WorldClim 2: New 1-km spatial resolution climate surfaces for global land areas. *International Journal of Climatology*, *37*(12), 4302–4315. https://doi.org/10.1002/joc.5086

Forster, P., Storelvmo, T., Armour, K., Collins, W., Dufresne, J.-L., Frame, D., et al. (2021). The Earth's energy budget, climate feedbacks and climate sensitivity. In V. Masson-Delmotte, P. Zhai, A. Pirani, S. L. Connors, C. Péan, S. Berger, et al. (Eds.), *Climate change 2021: The physical science basis. Contribution of working group I to the sixth assessment report of the intergovernmental panel on climate change* (pp. 923–1054). https://doi.org/10.1017/9781009157896.009.923

Fowler, R. A., Osburn, C. L., & Saros, J. E. (2020). Climate-driven changes in dissolved organic carbon and water Clarity in arctic lakes of west Greenland. *Journal of Geophysical Research: Biogeosciences*, *125*(2), 1–13. https://doi.org/10.1029/2019JG005170

Gentzel, T., Hershey, A. E., Rublee, P. A., & Whalen, S. C. (2012). Net sediment production of methane, distribution of methanogens and methane-oxidizing bacteria, and utilization of methane-derived carbon in an arctic lake. *Inland Waters*, *2*(2), 77–88. https://doi.org/10.5268/iw-2.2.416

Geological Survey of Norway. (2024). National bedrock database. Retrieved from https://geo.ngu.no/kart/berggrunn_mobil/?lang=eng

Geological Survey of Sweden. (2024). Berggrund 1:1 miljon. Retrieved from https://apps.sgu.se/kartvisare/kartvisare-berggrund-1-miljon.html

Grasset, C., Mendonça, R., Villamor Saucedo, G., Bastviken, D., Roland, F., & Sobek, S. (2018). Large but variable methane production in anoxic freshwater sediment upon addition of allochthonous and autochthonous organic matter. *Limnology & Oceanography*, *63*(4), 1488–1501. https://doi.org/10.1002/lno.10786

Grasset, C., Moras, S., Isidorova, A., Couture, R. M., Linkhorst, A., & Sobek, S. (2021). An empirical model to predict methane production in inland water sediment from particular organic matter supply and reactivity. *Limnology & Oceanography*, *66*(10), 3643–3655. https://doi.org/10.1002/lno.11905

Gudasz, C., Bastviken, D., Steger, K., Premke, K., Sobek, S., & Tranvik, L. J. (2010). Temperature-controlled organic carbon mineralization in lake sediments. *Nature*, *466*(7305), 478–481. https://doi.org/10.1038/nature09186

Håkanson, L. (1982). Bottom dynamics in lakes. In *Sediment/freshwater interaction: Proceedings of the second International Symposium held in Kingston, Ontario, 15–18 June 1981* (pp. 9–22). Springer.

Hastie, A., Lauerwald, R., Weyhenmeyer, G., Sobek, S., Verpoorter, C., & Regnier, P. (2018). CO2 evasion from boreal lakes: Revised estimate, drivers of spatial variability, and future projections. *Global Change Biology*, *24*(2), 711–728. https://doi.org/10.1111/gcb.13902

Heslop, J. K., Anthony, K. W., Grosse, G., Liebner, S., & Winkel, M. (2019). Century-scale time since permafrost thaw affects temperature sensitivity of net methane production in thermokarst-lake and talik sediments. *Science of the Total Environment*, *691*, 124–134. https://doi.org/10.1016/j.scitotenv.2019.06.402

Holgerson, M. A., & Raymond, P. A. (2016). Large contribution to inland water CO_2 and CH_4 emissions from very small ponds. *Nature Geoscience*, *9*(3), 222–226. https://doi.org/10.1038/ngeo2654

Huang, H., Wang, W., Lv, J., Liu, Q., Liu, X., Xie, S., et al. (2022). Relationship between chlorophyll a and environmental factors in lakes based on the random forest Algorithm. *Water (Switzerland)*, *14*(19), 1–11. https://doi.org/10.3390/w14193128

IPCC. (2021). *Climate change 2021: The physical science basis. Contribution of working group I to the sixth assessment report of the Intergovernmental panel on climate change*. Cambridge University Press.

Isidorova, A., Grasset, C., Mendonça, R., & Sobek, S. (2019). Methane formation in tropical reservoirs predicted from sediment age and nitrogen. *Scientific Reports*, *9*(1), 1–9. https://doi.org/10.1038/s41598-019-47346-7

Jähne, B., Heinz, G., & Dietrich, W. (1987). Measurement of the diffusion coefficients of sparingly soluble gases in water. *Journal of Geophysical Research*, *92*(C10), 10767–10776. https://doi.org/10.1029/JC092iC10p10767

Jakobsson, M., Mayer, L., Coakley, B., Dowdeswell, J. A., Forbes, S., Fridman, B., et al. (2012). The international bathymetric chart of the Arctic Ocean (IBCAO) version 3.0. *Geophysical Research Letters*, *39*(12), L12609. https://doi.org/10.1029/2012GL052219

Jansen, J., Thornton, B. F., Cortés, A., Snöälv, J., Wik, M., MacIntyre, S., & Crill, P. M. (2020). Drivers of diffusive CH 4 emissions from shallow subarctic lakes on daily to multi-year timescales. *Biogeosciences*, *17*(7), 1911–1932. https://doi.org/10.5194/bg-17-1911-2020

Jansson, M., Karlsson, J., & Jonsson, A. (2012). Carbon dioxide supersaturation promotes primary production in lakes. *Ecology Letters*, *15*(6), 527–532. https://doi.org/10.1111/j.1461-0248.2012.01762.x

Karlsson, J., Bystrom, P., Ask, J., Ask, P., Persson, L., & Jansson, M. (2009). Light limitation of nutrient-poor lake ecosystems. *Nature*, *460*(July), 23–27. https://doi.org/10.1038/nature08179

Kjellman, S. E., Thomas, E. K., Farnsworth, W. R., Cowling, O. C., Allaart, L., Brynjólfsson, S., & Schomacker, A. (2024). Seasonal precipitation variability on Svalbard inferred from Holocene sedimentary leaf wax δ2H. *Boreas*, *53*(3), 430–452. https://doi.org/10.1111/bor.12661

Klaus, M., Karlsson, J., & Seekell, D. (2021). Tree line advance reduces mixing and oxygen concentrations in arctic—Alpine lakes through wind sheltering and organic carbon supply. *Global Change Biology*, *27*(18), 1–16. https://doi.org/10.1111/gcb.15660

Kuhn, M. A., Varner, R. K., Bastviken, D., Crill, P., Macintyre, S., Turetsky, M., et al. (2021). BAWLD-CH4: A comprehensive dataset of methane fluxes from boreal and arctic ecosystems. *Earth System Science Data*, *13*(11), 5151–5189. https://doi.org/10.5194/essd-13-5151-2021

Langenegger, T., Vachon, D., Donis, D., & McGinnis, D. F. (2019). What the bubble knows: Lake methane dynamics revealed by sediment gas bubble composition. *Limnology & Oceanography*, *64*(4), 1526–1544. https://doi.org/10.1002/lno.11133

Lauerwald, R., Allen, G. H., Deemer, B. R., Liu, S., Maavara, T., Raymond, P., et al. (2023). Inland water greenhouse gas budgets for RECCAP2: 1. State-Of-The-Art of global scale assessments. *Global Biogeochemical Cycles*, *37*(5), 1–32. https://doi.org/10.1029/2022GB007657

Lenstra, W. K., Egger, M., Van Helmond, N. A. G. M., Kritzberg, E., Conley, D. J., & Slomp, C. P. (2018). Large variations in iron input to an oligotrophic Baltic Sea estuary: Impact on sedimentary phosphorus burial. *Biogeosciences*, *15*(22), 6979–6996. https://doi.org/10.5194/bg-15-6979-2018

Leppi, J. C., Arp, C. D., & Whitman, M. S. (2016). Predicting late winter dissolved oxygen levels in arctic lakes using Morphology and landscape Metrics. *Environmental Management*, *57*(2), 463–473. https://doi.org/10.1007/s00267-015-0622-x

Liaw, A., & Wiener, M. (2002). Classification and Regression by randomForest. *R News*, *2*(3), 18–22.

Lofton, D. D., Whalen, S. C., & Hershey, A. E. (2014). Effect of temperature on methane dynamics and evaluation of methane oxidation kinetics in shallow Arctic Alaskan lakes. *Hydrobiologia*, *721*(1), 209–222. https://doi.org/10.1007/s10750-013-1663-x

Martinez-Cruz, K., Sepulveda-Jauregui, A., Casper, P., Anthony, K. W., Smemo, K. A., & Thalasso, F. (2018). Ubiquitous and significant anaerobic oxidation of methane in freshwater lake sediments. *Water Research*, *144*(2), 332–340. https://doi.org/10.1016/j.watres.2018.07.053

McGowan, S., Anderson, N. J., Edwards, M. E., Hopla, E., Jones, V., Langdon, P. G., et al. (2018). Vegetation transitions drive the autotrophy-heterotrophy balance in Arctic lakes. *Limnology and Oceanography Letters*, *3*(3), 246–255. https://doi.org/10.1002/lol2.10086

McGowan, S., Anderson, N. J., Edwards, M. E., Langdon, P. G., Jones, V. J., Turner, S., et al. (2016). Long-term perspectives on terrestrial and aquatic carbon cycling from palaeolimnology. *Wiley Interdisciplinary Reviews: Water*, *3*(2), 211–234. https://doi.org/10.1002/wat2.1130

Meyer-Jacob, C., Michelutti, N., Paterson, A. M., Monteith, D., Yang, H., Weckström, J., et al. (2017). Inferring Past trends in lake water organic carbon concentrations in northern lakes using sediment spectroscopy. *Environmental Science and Technology*, *51*(22), 13248–13255. https://doi.org/10.1021/acs.est.7b03147

Michaud, A. B., & Apollonio, S. (2022). Overwinter oxygen and silicate dynamics in a high Arctic lake (Immerk lake, Devon Island, Canada). *Inland Waters*, *12*(3), 418–426. https://doi.org/10.1080/20442041.2022.2063623

Michelutti, N., & Smol, J. P. (2016). Visible spectroscopy reliably tracks trends in paleo-production. *Journal of Paleolimnology*, *56*(4), 253–265. https://doi.org/10.1007/s10933-016-9921-3

Michelutti, N., Wolfe, A. P., Vinebrooke, R. D., Rivard, B., & Briner, J. P. (2005). Recent primary production increases in arctic lakes. *Geophysical Research Letters*, *32*(19), 1–4. https://doi.org/10.1029/2005GL023693

Moras, S., Zellmer, U. R., Hiltunen, E., Grasset, C., & Sobek, S. (2024). Predicting methane formation rates of freshwater sediments in different climates. *Journal of Geophysical Research: Biogeosciences*, *129*, 1–17. https://doi.org/10.1029/2023JG007463

Natchimuthu, S., Sundgren, I., Gålfalk, M., Klemedtsson, L., Crill, P., Danielsson, Å., & Bastviken, D. (2016). Spatio-temporal variability of lake CH_4 fluxes and its influence on annual whole lake emission estimates. *Limnology & Oceanography*, *61*(S1), S13–S26. https://doi.org/10.1002/lno.10222

Nordi, K. Á., Thamdrup, B., & Schubert, C. J. (2013). Anaerobic oxidation of methane in an iron-rich Danish freshwater lake sediment. *Limnology & Oceanography*, *58*(2), 546–554. https://doi.org/10.4319/lo.2013.58.2.0546

Norwegian Polar Institute. (2014). Terrengmodell Svalbard (S0 Terrengmodell) [Dataset]. *Norwegian Polar Institute*. https://doi.org/10.21334/NPOLAR.2014.DCE53A47

Norwegian Mapping Authority. (2024). National Digital elevation model. Retrieved from https://www.hoydedata.no

Norwegian Polar Institute. (2024). GeoSvalbard. Retrieved from https://geokart.npolar.no/geologi/GeoSvalbard/#7/78.460/19.096

Nyman, M., Weckström, J., & Korhola, A. (2008). Chironomid response to environmental drivers during the Holocene in a shallow treeline lake in northwestern Fennoscandia. *The Holocene*, *18*(2), 215–227. https://doi.org/10.1177/0959683607086760

Olid, C., Rodellas, V., Rocher-Ros, G., Garcia-Orellana, J., Diego-Feliu, M., Alorda-Kleinglass, A., et al. (2022). Groundwater discharge as a driver of methane emissions from Arctic lakes. *Nature Communications*, *13*(1), 1–9. https://doi.org/10.1038/s41467-022-31219-1

Østby, T. I., Vikhamar Schuler, T., Ove Hagen, J., Hock, R., Kohler, J., & Reijmer, C. H. (2017). Diagnosing the decline in climatic mass balance of glaciers in Svalbard over 1957–2014. *The Cryosphere*, *11*(1), 191–215. https://doi.org/10.5194/tc-11-191-2017

Paasche, Ø., Løvlie, R., Dahl, S. O., Bakke, J., & Nesje, A. (2004). Bacterial magnetite in lake sediments: Late glacial to Holocene climate and sedimentary changes in northern Norway. *Earth and Planetary Science Letters*, *223*(3–4), 319–333. https://doi.org/10.1016/j.epsl.2004.05.001

Peeters, F., Encinas Fernandez, J., & Hofmann, H. (2019). Sediment fluxes rather than oxic methanogenesis explain diffusive CH_4 emissions from lakes and reservoirs. *Scientific Reports*, *9*(1), 1–10. https://doi.org/10.1038/s41598-018-36530-w

Pellerin, A., Lotem, N., Walter Anthony, K., Eliani Russak, E., Hasson, N., Røy, H., et al. (2022). Methane production controls in a young thermokarst lake formed by abrupt permafrost thaw. *Global Change Biology*, *28*(10), 3206–3221. https://doi.org/10.1111/gcb.16151

Rahalkar, M., Deutzmann, J., Schink, B., & Bussmann, I. (2009). Abundance and activity of methanotrophic bacteria in littoral and profundal sediments of lake constance (Germany). *Applied and Environmental Microbiology*, *75*(1), 119–126. https://doi.org/10.1128/AEM.01350-08

Rantanen, M., Karpechko, A. Y., Lipponen, A., Nordling, K., Hyvärinen, O., Ruosteenoja, K., et al. (2022). The Arctic has warmed nearly four times faster than the globe since 1979. *Communications Earth & Environment*, *3*(1), 1–10. https://doi.org/10.1038/s43247-022-00498-3

Rasmussen, H., Bondevik, S., & Corner, G. D. (2018). Holocene relative sea level history and Storegga tsunami run-up in Lyngen, northern Norway. *Journal of Quaternary Science*, *33*(4), 393–408. https://doi.org/10.1002/jqs.3021

R Core Team. (2024). *R: A language and environment for statistical computing*. R Foundation for Statistical Computing. Retrieved from https://www.R-project.org/

Rissanen, A. J., Jilbert, T., Simojoki, A., Mangayil, R., Aalto, S. L., Khanongnuch, R., et al. (2023). Methane-related microbial communities in lake sediments. *Environmental Microbiology*, *11*(5), 1–15. https://doi.org/10.1128/spectrum.01955-23

Schuur, E. A. G., McGuire, A. D., Schädel, C., Grosse, G., Harden, J. W., Hayes, D. J., et al. (2015). Climate change and the permafrost carbon feedback. *Nature*, *520*(7546), 171–179. https://doi.org/10.1038/nature14338

Schwarz, J. I. K., Eckert, W., & Conrad, R. (2008). Response of the methanogenic microbial community of a profundal lake sediment (Lake Kinneret, Israel) to algal deposition. *Limnology & Oceanography*, *53*(1), 113–121. https://doi.org/10.4319/lo.2008.53.1.0113

Seekell, D. A., Lapierre, J.-F., Ask, J., Bergstrom, A.-K., Deininger, A., Rodriguez, P., & Karlsson, J. (2015). The influence of dissolved organic carbon on primary production in northern lakes. *Limnology & Oceanography*, *60*(4), 1276–1285. https://doi.org/10.1002/lno.10096

seNorge.no. (2024). Klima. Retrieved from http://www.senorge.no/

Simon, S. M., Glaum, P., & Valdovinos, F. S. (2023). Interpreting random forest analysis of ecological models to move from prediction to explanation. *Scientific Reports*, *13*(1), 1–12. https://doi.org/10.1038/s41598-023-30313-8

Solomon, C. T., Bruesewitz, D. A., Richardson, D. C., Rose, K. C., Bogert, C. V. D., Hanson, P. C., et al. (2013). Ecosystem respiration: Drivers of daily variability and background respiration in lakes around the globe. *Limnology & Oceanography*, *58*(3), 849–866. https://doi.org/10.4319/lo.2013.58.3.0849

Swedish Meteorological and Hydrological Institute. (2024). Smhi. Retrieved from https://www.smhi.se

Thottathil, S. D., Reis, P. C. J., & Prairie, Y. T. (2022). Magnitude and drivers of oxic methane production in small temperate lakes. *Environmental Science and Technology*, *56*(15), 11041–11050. https://doi.org/10.1021/acs.est.2c01730

Vachon, D., Langenegger, T., Donis, D., & McGinnis, D. F. (2019). Influence of water column stratification and mixing patterns on the fate of methane produced in deep sediments of a small eutrophic lake. *Limnology & Oceanography*, *64*(5), 2114–2128. https://doi.org/10.1002/lno.11172

van Grinsven, S., Meier, D. V., Michel, A., Han, X., Schubert, C. J., & Lever, M. A. (2022). Redox zone and trophic state as drivers of methane-oxidizing bacterial abundance and community structure in lake sediments. *Frontiers in Environmental Science*, *10*, 857358. https://doi.org/10.3389/fenvs.2022.857358

Voldstad, L. H., Alsos, I. G., Farnsworth, W. R., Heintzman, P. D., Håkansson, L., Kjellman, S. E., et al. (2020). A complete Holocene lake sediment ancient DNA record reveals long-standing high Arctic plant diversity hotspot in northern Svalbard. *Quaternary Science Reviews*, *234*, 106207. https://doi.org/10.1016/j.quascirev.2020.106207

Walker, D. A., Raynolds, M. K., Daniëls, F. J., Einarsson, E., Elvebakk, A., Gould, W. A., et al. (2005). The circumpolar Arctic vegetation map. *Journal of Vegetation Science*, *16*(3), 267–282. https://doi.org/10.1111/j.1654-1103.2005.tb02365.x

Weiss, M., & Banko, G. (2018). Ecosystem type map v3.1—Terrestrial and marine ecosystems. December 2018, 78. Retrieved from https://www.eionet.europa.eu/etcs/etc-bd/products/etc-bd-reports/ecosystem_mapping_v3_1

West, W. E., Coloso, J. J., & Jones, S. E. (2012). Effects of algal and terrestrial carbon on methane production rates and methanogen community structure in a temperate lake sediment. *Freshwater Biology*, *57*(5), 949–955. https://doi.org/10.1111/j.1365-2427.2012.02755.x

West, W. E., Mccarthy, S. M., & Jones, S. E. (2015). Phytoplankton lipid content influences freshwater lake methanogenesis. *Freshwater Biology*, *60*(11), 2261–2269. https://doi.org/10.1111/fwb.12652

Whiticar, M. J. (1996). Isotope tracking of microbial methane formation and oxidation. *Internationale Vereinigung für Theoretische und Angewandte Limnologie: Mitteilungen*, *25*(1), 39–54. https://doi.org/10.1080/05384680.1996.11904065

Whiticar, M. J., & Faber, E. (1986). Methane oxidation in sediment and water column environments-Isotope evidence. *Organic Geochemistry*, *10*(4–6), 759–768. https://doi.org/10.1016/S0146-6380(86)80013-4

Wik, M., Varner, R. K., Anthony, K. W., MacIntyre, S., & Bastviken, D. (2016). Climate-sensitive northern lakes and ponds are critical components of methane release. *Nature Geoscience*, *9*(2), 99–105. https://doi.org/10.1038/ngeo2578

Wilkinson, J., Maeck, A., Alshboul, Z., & Lorke, A. (2015). Continuous seasonal river ebullition measurements linked to sediment methane formation. *Environmental Science and Technology*, *49*(22), 13121–13129. https://doi.org/10.1021/acs.est.5b01525

Yvon-Durocher, G., Allen, A. P., Bastviken, D., Conrad, R., Gudasz, C., St-Pierre, A., et al. (2014). Methane fluxes show consistent temperature dependence across microbial to ecosystem scales. *Nature*, *507*(7493), 488–491. https://doi.org/10.1038/nature13164

References From the Supporting Information

Adams, D. D., Matisoff, G., & Snodgrass, W. J. (1982). Flux of reduced chemical constituents (Fe^{2+}, Mn^{2+}, NH_4^+ and CH_4) and sediment oxygen demand in Lake Erie. *Hydrobiologia*, *91–92*(1), 405–414. https://doi.org/10.1007/bf02391956

Adler, M., Eckert, W., & Sivan, O. (2011). Quantifying rates of methanogenesis and methanotrophy in Lake Kinneret sediments (Israel) using pore-water profiles. *Limnology & Oceanography*, *56*(4), 1525–1535. https://doi.org/10.4319/lo.2011.56.4.1525

Bartosiewicz, M., Maranger, R., Przytulska, A., & Laurion, I. (2021). Effects of phytoplankton blooms on fluxes and emissions of greenhouse gases in a eutrophic lake. *Water Research*, *196*, 116985. https://doi.org/10.1016/j.watres.2021.116985

Bastviken, D., Cole, J. J., Pace, M. L., & Bogert, M. C. V. D. (2008). Fates of methane from different lake habitats: Connecting whole-lake budgets and CH_4 emissions. *Journal of Geophysical Research*, *113*(May), 1–13. https://doi.org/10.1029/2007JG000608

Bastviken, D., Cole, J., Pace, M., & Tranvik, L. J. (2004). Methane emissions from lakes: Dependence of lake characteristics, two regional assessments, and a global estimate. *Global Biogeochemical Cycles*, *18*(4), 1–12. https://doi.org/10.1029/2004GB002238

Bédard, C., & Knowles, R. (1991). Hypolimnetic O_2 consumption, denitrification, and methanogenesis in a thermally stratified lake. *Canadian Journal of Fisheries and Aquatic Sciences*, *48*(6), 1048–1054. https://doi.org/10.1139/f91-123

Buchholz, L. A., Klump, J. V., Lynne, M., Collins, P., Brantner, C. A., & Remsen, C. C. (1995). Activity of methanotrophic bacteria in Green Bay sediments. *FEMS Microbiology Ecology*, *16*, 1–8. https://doi.org/10.1111/j.1574-6941.1995.tb00262.x

Bussmann, I., & Schink, B. (2006). A modified diffusion-based methane sensor and its application in freshwater sediment. *Limnology and Oceanography: Methods*, *4*(8), 275–283. https://doi.org/10.4319/lom.2006.4.275

Carignan, R., & Lean, D. R. S. (1991). Regeneration of dissolved substances in a seasonally anoxic lake: The relative importance of processes occurring in the water column and in the sediments. *Limnology & Oceanography*, *36*(4), 683–707. https://doi.org/10.4319/lo.1991.36.4.0683

Cunada, C. L. (2016). *Seasonal methane dynamics in lakes of the Mackenzie river Delta, Western Canadian arctic (Master's thesis)*. Simon Fraser University. Retrieved from http://summit.sfu.ca/item/16714

Donis, D., Flury, S., Stöckli, A., Spangenberg, J. E., Vachon, D., & McGinnis, D. F. (2017). Full-scale evaluation of methane production under oxic conditions in a mesotrophic lake. *Nature Communications*, *8*(1), 1–11. https://doi.org/10.1038/s41467-017-01648-4

Durisch-Kaiser, E., Schmid, M., Peeters, F., Kipfer, R., Dinkel, C., Diem, T., et al. (2011). What prevents outgassing of methane to the atmosphere in Lake Tanganyika? *Journal of Geophysical Research*, *116*, 1–16. https://doi.org/10.1029/2010JG001323

Fahrner, S., Radke, M., Karger, D., & Blodau, C. (2008). Organic matter mineralisation in the hypolimnion of an eutrophic Maar lake. *Aquatic Sciences*, *70*(3), 225–237. https://doi.org/10.1007/s00027-008-8008-2

Fallon, R. D., Harrits, S., Hanson, R. S., & Brock, T. D. (1980). The role of methane in internal carbon cycling in Lake Mendota during summer stratification. *Limnology & Oceanography*, *25*(2), 357–360. https://doi.org/10.4319/lo.1980.25.2.0357

Gu, B., Schelske, C. L., & Hodell, D. A. (2004). Extreme ^{13}C enrichments in a shallow hypereutrophic lake: Implications for carbon cycling. *Limnology & Oceanography*, *49*(4 I), 1152–1159. https://doi.org/10.4319/lo.2004.49.4.1152

Hartmann, J. F., Gu, M., Klintzsch, T., Kirillin, G., Grossart, H., Keppler, F., & Isenbeck-schro, M. (2020). High Spatiotemporal dynamics of methane production and emission in oxic surface water. *Environmental Science & Technology Journal*, *54*(3), 1451–1463. https://doi.org/10.1021/acs.est.9b03182

Howard, D. L., Frea, J. I., & Pfister, R. M. (1971). The potential for methane carbon cycling in Lake Erie. In *Paper presented at 14th Conference on Great lakes Research, International Assoc. Of Great lakes Res., Ann Arbor, Mich*.

Huttunen, J. T., Väisänen, T. S., Hellsten, S. K., & Martikainen, P. J. (2006). Methane fluxes at the sediment-water interface in some boreal lakes and reservoirs. *Boreal Environment Research*, *11*(1), 27–34.

Iversen, N., Oremland, R. S., & Klug, M. J. (1987). Big Soda Lake (Nevada). 3. Pelagic methanogenesis and anaerobic methane oxidation. *Limnology & Oceanography*, *32*(4), 804–814. https://doi.org/10.4319/lo.1987.32.4.0804

Jones, J. G., & Simon, B. M. (1981). Differences in microbial Decomposition processes in profundal and littoral lake sediments, with particular reference to the nitrogen cycle. *Journal of General Microbiology*, *123*(198 I), 297–312. https://doi.org/10.1099/00221287-123-2-297

Kelly, C. A., & Chynoweth, D. P. (1980). Comparison of in situ and in Vitro rates of methane release in freshwater sediments. *Applied and Environmental Microbiology*, *40*(2), 287–293. https://doi.org/10.1128/aem.40.2.287-293.1980

Kelly, C. A., & Chynoweth, P. (1981). The contributions of temperature and of the input of organic matter in controlling rates of sediment methanogenesis. *Limnology & Oceanography*, *26*(5), 891–897. https://doi.org/10.4319/lo.1981.26.5.0891

Koschorreck, M., Wendt-potthoff, K., Scharf, B., & Richnow, H. H. (2008). Methanogenesis in the sediment of the acidic lake Caviahue in Argentina. *Journal of Volcanology and Geothermal Research*, *178*(2), 197–204. https://doi.org/10.1016/j.jvolgeores.2008.06.017

Kuivila, K. M., Murray, J. W., Devol, A. H., Lidstrom, M. E., & Reimers, C. E. (1988). Methane cycling in the sediments of Lake Washington. *Limnology & Oceanography*, *33*(4), 571e581. https://doi.org/10.4319/lo.1988.33.4.0571

Li, L., Fuchs, A., Herrero, S., Xue, B., & Casper, P. (2021). Science of the Total Environment Spatial methane pattern in a deep freshwater lake: Relation to water depth and topography. *Science of the Total Environment*, *764*, 142829. https://doi.org/10.1016/j.scitotenv.2020.142829

Li, L., Xue, B., Yao, S., Tao, Y., & Yan, R. (2018). Spatial—Temporal patterns of methane dynamics in Lake Taihu. *Hydrobiologia*, *822*(1), 143–156. https://doi.org/10.1007/s10750-018-3670-4

Matthews, D. A., Effler, S. W., & Matthews, C. M. (2005). Long-term trends in methane flux from the sediments of Onondaga Lake, NY: Sediment diagenesis and impacts on dissolved oxygen resources. *Archiv für Hydrobiologie*, *163*(4), 435–462. https://doi.org/10.1127/0003-9136/2005/0163-0435

Muller, B., Bryant, L. D., Matzinger, A., & Wuest, A. (2012). Hypolimnetic oxygen depletion in eutrophic lakes. *Environmental Science & Technology*, *46*(18), 9964–9971. https://doi.org/10.1021/es301422r

Oremland, R. S., Miller, L. G., Whiticar, M. J., Survey, U. S. G., & Park, M. (1987). Sources and flux of natural gases from Mono Lake, California. *Geochimica et Cosmochimica Acta*, *51*(11), 2915–2929. https://doi.org/10.1016/0016-7037(87)90367-x

Pasche, N., Schmid, M., Vazquez, F., Schubert, C. J., Wüest, A., Kessler, J. D., et al. (2011). Methane sources and sinks in lake Kivu. *Journal of Geophysical Research*, *116*(G3), 1–16. https://doi.org/10.1029/2011JG001690

Pedrozo, F. L., Temporetti, P. F., Beamud, G., & Diaz, M. M. (2008). Volcanic nutrient inputs and trophic state of Lake Caviahue, Patagonia, Argentina. *Journal of Volcanology and Geothermal Research*, *178*(2), 205–212. https://doi.org/10.1016/j.jvolgeores.2008.06.018

Pekkarinen, M. (1990). Comprehensive survey of the hyper-trophic lake Tuusulanjärvi: Nutrient loading, water quality and prospects of restoration. *Aqua Fennica*, *20*, 13–25.

Puro, A., Väisänen, T., Juntura, E., Hätälä, E., Hiltunen, E., & Halonen, M. (1999). Ranuanjärven, Takajärven ja Luiminkajärven tila ja kunnostusmahdollisuudet. *Alueelliset ympäristöjulkaisut*, *88*.

Randlett, M. E., Sollberger, S., DelSontro, T., Müller, B., Corella, J. P., Wehrli, B., & Schubert, C. J. (2015). Mineralization pathways of organic matter deposited in a river-lake transition of the Rhone River Delta, Lake Geneva. *Environmental Sciences: Processes & Impacts*, *17*(2), 370–380. https://doi.org/10.1039/c4em00470a

Rudd, J. W. M., & Hamilton, R. D. (1978). Methane cycling in a eutrophic shield lake and its effects on whole lake metabolism. *Limnology & Oceanography*, *23*(2), 337–348. https://doi.org/10.4319/lo.1978.23.2.0337

Schubert, C. J., Vazquez, F., Losekann-Behrens, T., Knittel, K., Tonolla, M., & Boetius, A. (2011). Evidence for anaerobic oxidation of methane in sediments of a freshwater system (Lago di Cadagno). *FEMS Microbiology Ecology*, *76*(1), 26–38. https://doi.org/10.1111/j.1574-6941.2010.01036.x

Sobek, S., Anderson, N. J., Bernasconi, S. M., & DelSontro, T. (2014). Low organic carbon burial efficiency in arctic lake sediments. *Journal of Geophysical Research: Biogeosciences*, *119*(6), 1231–1243. https://doi.org/10.1002/2014JG002612

Sobek, S., Durisch-Kaiser, E., Zurbrügg, R., Wongfun, N., Wessels, M., Pasche, N., & Wehrli, B. (2009). Organic carbon burial efficiency in lake sediments controlled by oxygen exposure time and sediment source. *Limnology & Oceanography*, *54*(6), 2243–2254. https://doi.org/10.4319/lo.2009.54.6.2243

Steinsberger, T., Schmid, M., Wüest, A., Schwefel, R., Wehrli, B., & Müller, B. (2017). Organic carbon mass accumulation rate regulates the flux of reduced substances from the sediments of deep lakes. *Biogeosciences*, *14*(13), 3275–3285. https://doi.org/10.5194/bg-14-3275-2017

Strayer, R. F., & Tiedje, J. M. (1978). Kinetic parameters of the conversion of methane precursors to methane in a hypereutrophic lake sediment. *Applied and Environmental Microbiology*, *36*(2), 330–340. https://doi.org/10.1128/aem.36.2.330-340.1978

Thottathil, S. D., & Prairie, Y. T. (2021). Coupling of stable carbon isotopic signature of methane and ebullitive fluxes in northern temperate lakes. *Science of the Total Environment*, *777*, 146117. https://doi.org/10.1016/j.scitotenv.2021.146117

Thottathil, S. D., Reis, P. C. J., del Giorgio, P. A., & Prairie, Y. T. (2018). The extent and regulation of summer methane oxidation in northern lakes. *Journal of Geophysical Research: Biogeosciences*, *123*(10), 3216–3230. https://doi.org/10.1029/2018JG004464

Urban, N. R., Dinkel, C., & Wehrli, B. (1997). Solute transfer across the sediment surface of a eutrophic lake: I. Porewater profiles from dialysis samplers. *Aquatic Sciences*, *59*, 1–25. https://doi.org/10.1007/pl00001302